

The Riemann problem for a generalized Burgers equation with spatially decaying sound speed

Needham, David; Meyer, John; Billingham, John; Drysdale, Catherine

DOI:

[10.1111/sapm.12561](https://doi.org/10.1111/sapm.12561)

License:

Creative Commons: Attribution (CC BY)

Document Version

Publisher's PDF, also known as Version of record

Citation for published version (Harvard):

Needham, D, Meyer, J, Billingham, J & Drysdale, C 2023, 'The Riemann problem for a generalized Burgers equation with spatially decaying sound speed: I Large-time asymptotics', *Studies in Applied Mathematics*, vol. 150, no. 4, pp. 963-995. <https://doi.org/10.1111/sapm.12561>

[Link to publication on Research at Birmingham portal](#)

General rights

Unless a licence is specified above, all rights (including copyright and moral rights) in this document are retained by the authors and/or the copyright holders. The express permission of the copyright holder must be obtained for any use of this material other than for purposes permitted by law.

- Users may freely distribute the URL that is used to identify this publication.
- Users may download and/or print one copy of the publication from the University of Birmingham research portal for the purpose of private study or non-commercial research.
- User may use extracts from the document in line with the concept of 'fair dealing' under the Copyright, Designs and Patents Act 1988 (?)
- Users may not further distribute the material nor use it for the purposes of commercial gain.

Where a licence is displayed above, please note the terms and conditions of the licence govern your use of this document.

When citing, please reference the published version.

Take down policy

While the University of Birmingham exercises care and attention in making items available there are rare occasions when an item has been uploaded in error or has been deemed to be commercially or otherwise sensitive.

If you believe that this is the case for this document, please contact UBIRA@lists.bham.ac.uk providing details and we will remove access to the work immediately and investigate.

The Riemann problem for a generalized Burgers equation with spatially decaying sound speed. I Large-time asymptotics

David J. Needham¹ | John C. Meyer¹  | John Billingham² | Catherine Drysdale³

¹School of Mathematics, University of Birmingham, Birmingham, UK

²School of Mathematical Sciences, University of Nottingham, Nottingham, UK

³ForBetterHealth, Clarksdale, Mississippi, USA

Correspondence

David J. Needham, School of Mathematics, University of Birmingham, Birmingham B15 2TT, UK.

Email: d.j.needham@bham.ac.uk

Abstract

In this paper, we consider the classical Riemann problem for a generalized Burgers equation,

$$u_t + h_\alpha(x)uu_x = u_{xx},$$

with a spatially dependent, nonlinear sound speed, $h_\alpha(x) \equiv (1 + x^2)^{-\alpha}$ with $\alpha > 0$, which decays algebraically with increasing distance from a fixed spatial origin. When $\alpha = 0$, this reduces to the classical Burgers equation. In this first part of a pair of papers, we focus attention on the large-time structure of the associated Riemann problem, and obtain its detailed structure, as $t \rightarrow \infty$, via the method of matched asymptotic coordinate expansions (this uses the classical method of matched asymptotic expansions, with the asymptotic parameters being the independent coordinates in the evolution problem; this approach is developed in detail in the monograph of Leach and Needham, as referenced in the text), over all parameter ranges. We identify a significant bifurcation in structure at $\alpha = \frac{1}{2}$.

This is an open access article under the terms of the [Creative Commons Attribution](https://creativecommons.org/licenses/by/4.0/) License, which permits use, distribution and reproduction in any medium, provided the original work is properly cited.

© 2023 The Authors. *Studies in Applied Mathematics* published by Wiley Periodicals LLC.

KEYWORDS

generalized Burgers equation, large-time structure, Riemann problem, spatially decaying sound speed

1 | INTRODUCTION

In this paper and its companion, we investigate the effects of a spatially varying nonlinear sound speed in a generalized form of the classical Burgers equation. Specifically, we consider the situation when the nonlinear sound speed decays algebraically with increasing spatial distance. A discussion of generalized Burgers equations, and their significance in nonlinear acoustics, in the present context, can be found in the papers by, among many others^{2–7} and,⁸ and very recently,⁹ together with the classical texts of Whitham,¹⁰ and Rudenko and Soluyan.¹¹ A number of recent papers have addressed (using, among other approaches, Cole–Hopf type transformations, similarity and separable structures, and ad hoc approximations) the generalized Burgers equation, with time-dependent viscosity,¹² and linear damping,¹³ while the inclusion of a forcing term is considered in Refs. [14] and [15]. Higher-dimensional considerations are made in Ref. [16], while the Burgers/KdV fusion is addressed in Ref. [17]. In relation to nonlinear acoustics, the spatially decaying sound speed considered here represents finite amplitude sound propagation in a spatially varying, inhomogeneous medium, in which, relative to the constant background sound speed, the propagation of finite amplitude acoustic disturbances has sound speed $c(u, x) = \phi(x)u + O(u^2)$ as $u \rightarrow 0$, with u being the dimensionless acoustic disturbance and x measuring dimensionless distance from a fixed origin. The function $\phi(x)$ measures the inhomogeneous local variation of the finite amplitude sound speed in the material background. Qualitatively, this type of spatially decaying inhomogeneity in the local sound speed could be effected in, for example, a long tube of gaseous material which has a prescribed background local density which is bounded and decreases with distance, from a local maximum at the spatial origin. To model this situation, we make a specific choice of spatial variation in the local sound speed. This choice is motivated by a number of observations. First, it is a generic representative for any smoothly decreasing variation which decays algebraically with distance at long range. Second, for any more general decreasing variations which decay more rapidly with distance than algebraically, the results here obtained will provide upper bounds, via the parabolic comparison theorem. Our aim is, therefore, to develop a detailed analysis of the Riemann problem associated with this class of generalized, spatially inhomogeneous, Burgers equation.

It is convenient to introduce here the set $D_T \subset \mathbb{R}^2$, which, for given $T > 0$, is defined as:

$$D_T = \{(x, t) : (x, t) \in \mathbb{R} \times (0, T)\}, \quad (1)$$

with closure \overline{D}_T . A further notational convenience that we will use extensively throughout the paper is writing $f \geq O(g)^+$ to indicate that $f = O(g)$ or $f \gg O(g)$, with $f > 0$, and similarly $f \leq O(g)^+$ indicates $f = O(g)$ or $f \ll O(g)$, with $f > 0$. When the superscript $+$ is replaced by the superscript $-$, the same definition carries over *except now* $f > 0$ is replaced by $f < 0$. In the same vein, $f = O(g)^+$ indicates that $f = O(g)$ and $f > 0$, while $f = O(g)^-$ correspondingly indicates

that again $f = O(g)$ and now $f < 0$. We now consider the Cauchy problem for $u : D_T \rightarrow \mathbb{R}$ given by:

$$u \in L^\infty(D_T) \cap C^{2,1}(D_T), \quad (2)$$

$$u_t + h_\alpha(x)uu_x = u_{xx} \text{ on } D_T, \quad (3)$$

$$u(x, t) = \int_{-\infty}^{\infty} \frac{u_0(s)}{\sqrt{4\pi t}} e^{-\frac{(s-x)^2}{4t}} ds + O(t) \text{ as } t \rightarrow 0^+, \quad (4)$$

uniformly for $x \in \mathbb{R}$. Here, for a given $\alpha > 0$, $h_\alpha : \mathbb{R} \rightarrow \mathbb{R}$ is given by:

$$h_\alpha(x) = \frac{1}{(1+x^2)^\alpha} \quad \forall x \in \mathbb{R}, \quad (5)$$

while $u_0 : \mathbb{R} \rightarrow \mathbb{R}$ is the prescribed initial data, which is Lebesgue measurable, with $u_0 \in L^\infty(\mathbb{R})$. We denote the Cauchy problem given by (2)–(5) as (BIVP). It should be noted that, via (4), at each $x \in \mathbb{R}$ at which u_0 is continuous, then $u(x, t) \rightarrow u_0(x)$ as $t \rightarrow 0^+$. Moreover, when u_0 is continuous for $x \in [x_1, x_2]$ ($x_1 > x_2$), then $u(x, t) \rightarrow u_0(x)$ as $t \rightarrow 0^+$, uniformly for $x \in [x_1, x_2]$. In relation to applications, we may consider the generalized, spatially inhomogeneous Burgers equation in (3) as representing a rational model for the unidirectional propagation of a transitional, weakly non-linear acoustic wave through a viscous medium with a spatially varying local sound speed, which is weakly decaying with distance, from a localized maximum. In this paper, we focus attention on the Riemann problem for the Burgers equation (3), and thus we consider (BIVP) when the initial data $u_0 : \mathbb{R} \rightarrow \mathbb{R}$ has the specific form:

$$u_0(x) = \begin{cases} u^+ & \text{for } x > 0, \\ u^- & \text{for } x \leq 0, \end{cases} \quad (6)$$

with $u^+, u^- \in \mathbb{R}$ and $u^+ \neq u^-$. On using (6), condition (4) can be written as:

$$u(x, t) = u^+ - \frac{1}{2}(u^+ - u^-) \operatorname{erfc}\left(\frac{x}{2\sqrt{t}}\right) + O(t) \text{ as } t \rightarrow 0^+, \quad (7)$$

uniformly for $x \in \mathbb{R}$. The aim of the present paper is to examine in detail the large- t structure of the Riemann problem given by (BIVP) with (7). Generic qualitative results relating to the more general form of (BIVP) will be presented in the second of this pair of papers. At this stage, it is instructive to simply quote the results from this second paper, as they apply to (BIVP) with the specific initial data (7), and as they apply to the objectives of the current paper. Specifically, we can summarize these results in the following:

Theorem 1. *There exists a global solution $u : D_\infty \rightarrow \mathbb{R}$ to (BIVP). This solution is unique. In addition, for each $T > 0$, the solution depends continuously on the parameters u^+ and u^- , in D_T . Also, for each $T > 0$, $u(x, t) \rightarrow u^\pm$ as $x \rightarrow \pm\infty$, uniformly for $t \in (0, T]$, while $u_x(\cdot, t) > 0 (< 0)$ when $u^- < u^+ (u^- > u^+)$ for all $t \in (0, \infty)$.*

A proof of this theorem follows directly from Proposition 2.8 and Proposition 2.9 in the second of this pair of papers,¹⁸ henceforth referred to as (MNII). To reduce the region of the (u^+, u^-) parameter space that we need to investigate, we also have:

Corollary 1. For $(u^+, u^-) \in \mathbb{R}^2$, let the corresponding unique, global solution to (BIVP) be denoted by $u = U(\cdot, \cdot, u^+, u^-)$. Then, for each $(x, t) \in D_\infty$,

$$U(x, t, -u^-, -u^+) = -U(-x, t, u^+, u^-). \quad (8)$$

Proof. This follows on observing the invariance of the PDE (3) under the transformation $(x, u) \mapsto (-x, -u)$, together with the uniqueness property established in Theorem 1 for (BIVP). ■

As a consequence of this result, we need only to investigate (BIVP) for $(u^+, u^-) \in \mathcal{H}$, with

$$\mathcal{H} = \{(u^+, u^-) \in \mathbb{R}^2 : u^- \geq -u^+\}. \quad (9)$$

In addition, we note that when $(u^+, u^-) = (u^+, -u^+)$, it is an immediate consequence of (8) that the corresponding solution to (BIVP) is an odd function of the spatial variable x .

As stated earlier, the specific objective of the present paper is the determination of the detailed large- t asymptotic structure of the solution to the problem (BIVP), with particular attention being paid to the key attracting features in the solution as $t \rightarrow \infty$, and how these key features depend upon the parameters $\alpha > 0$ and $(u^+, u^-) \in \mathcal{H}$. To achieve this, we adopt the method of matched asymptotic coordinate expansions, as developed by Leach and Needham,¹ which, specifically, has been successful in similar applications to Riemann-type problems for classes of temporally inhomogeneous, generalized Burgers equations (see, e.g., Refs. [7] and [8]). Briefly, this approach uses the classical method of matched asymptotic expansions, but with the independent coordinates as the asymptotic parameters. This involves first constructing the asymptotic solution as $t \rightarrow 0^+$, uniformly for $x \in \mathbb{R}$; this is then used, via matching, to construct the asymptotic solution as $x \rightarrow \pm\infty$ with $t = O(1)^+$, respectively; this then provides, again via matching, the far field information required to enable the key asymptotic structure as $t \rightarrow \infty$, uniformly for $x \in \mathbb{R}$, to be fully determined. We find that there is a significant bifurcation in the large- t structure for (BIVP) as α passes through the critical value $\alpha = \alpha_c = \frac{1}{2}$. For $\alpha \in (0, \frac{1}{2})$, the key structure is a decelerating viscous shock wave ($u^+ < u^-$) or a decelerating expansion wave ($u^+ > u^-$), while, for $\alpha \in (\frac{1}{2}, \infty)$, the key structure is a diffusion dominated, stationary stretching front, in all cases. It is further established that the critical case $\alpha = \frac{1}{2}$ can fall into either the diffusion front case or the expansion/shock wave case depending on the magnitudes of the parameters u^- and u^+ .

The paper is constructed as follows. In Section 2, we begin the analysis by developing the small- t asymptotic structure to (BIVP). Section 3 then uses the details obtained in Section 2 to develop the asymptotic structure to (BIVP) as $x \rightarrow \pm\infty$. Finally, in Sections 4–6, the detailed asymptotic structure to (BIVP) can be developed as $t \rightarrow \infty$, guided by the details from Section 3. In each section, illustrative numerical solutions are provided, for comparison with the asymptotic results. A discussion is presented in Section 7.

2 | ASYMPTOTIC SOLUTION AS $t \rightarrow 0^+$

In this section, we construct the asymptotic solution to (BIVP) as $t \rightarrow 0^+$, uniformly for $x \in \mathbb{R}$. When t is small, the form of the initial data, and a balancing of terms in Equation (3) so as to retain the diffusion term to smooth out the initial discontinuity in the initial data, leads to a structure which has three asymptotic regions (a central smoothing region, together with left and right far field connecting regions), as follows:

Region I: $x = O(t^{\frac{1}{2}})$ and $u = O(1)$ as $t \rightarrow 0^+$

In this region, we introduce the scaled coordinate $\eta = x/t^{\frac{1}{2}} = O(1)$ as $t \rightarrow 0^+$, and expand in the form:

$$u(\eta, t) = \bar{u}(\eta) + O(t) \text{ as } t \rightarrow 0^+, \quad (10)$$

with $\eta = O(1)$. After writing (3) in terms of the scaled variables, substituting from (10) and applying condition (7), we readily obtain, after an integration,

$$\bar{u}(\eta) = u^+ - \frac{1}{2}(u^+ - u^-)\operatorname{erfc}\left(\frac{1}{2}\eta\right) \quad \forall \eta \in \mathbb{R}. \quad (11)$$

We note that the parameter α does not appear at leading order in this region. We now move on to complete the asymptotic structure with the two additional outer regions when $(\pm)x \geq O(1)$, respectively.

Region II⁺: $x \geq O(1)^+$ and $u = u^+ + o(1)$ as $t \rightarrow 0^+$

An examination of (10) and (11) when $\eta \gg 1$ determines that we must write,

$$u(x, t) = u^+ - (u^+ - u^-)\exp(-\phi(x, t)t^{-1}), \quad (12)$$

and expand in the form,

$$\phi(x, t) = \phi_0(x) + \phi_1(x)t \log t + \phi_2(x)t + o(t) \text{ as } t \rightarrow 0^+ \quad (13)$$

with $x \geq O(1)^+$. After substitution from (12) and (13) into (3), expanding, solving at each order in turn, together with asymptotic matching to region I as $x \rightarrow 0^+$, we obtain,

$$\phi_0(x) = \frac{1}{4}x^2, \quad \phi_1(x) = -\frac{1}{2}, \quad (14)$$

$$\phi_2(x) = \log x + \frac{1}{2} \log \pi - \frac{1}{2}u^+ \int_0^x (1+s^2)^{-\alpha} ds, \quad (15)$$

for $x > 0$.

Region II⁻: $(-x) \geq O(1)^+$ and $u = u^- + o(1)$ as $t \rightarrow 0^+$

Again, it follows directly from (10) and (11), with $(-\eta) \gg 1$, that we must write,

$$u(x, t) = u^- + (u^+ - u^-) \exp(-\psi(x, t)t^{-1}), \quad (16)$$

and again expand in a similar form to (13). Without giving details, we readily obtain the expansion,

$$\psi(x, t) = \frac{1}{4}x^2 - \frac{1}{2}t \log t + (\log(-x) + \frac{1}{2} \log \pi + \frac{1}{2}u^- \int_x^0 (1+s^2)^{-\alpha} ds)t + o(t) \text{ as } t \rightarrow 0^+, \quad (17)$$

with $x \leq O(1)^-$.

The asymptotic solution to (BIVP) as $t \rightarrow 0^+$ is now complete, and can be used to assist in constructing the asymptotic forms for (BIVP) as $x \rightarrow \pm\infty$, with $t = O(1)^+$.

3 | ASYMPTOTIC SOLUTION AS $x \rightarrow \pm\infty$

This section constructs the asymptotic solution to (BIVP) as $x \rightarrow \pm\infty$ with $t = O(1)^+$. The form of the expansions here are obtained directly from the corresponding expansions in regions II^\pm , respectively, when considered with $|x|$ large and $t = O(1)^+$. Without presenting details, which are standard, we obtain, after matching with regions II^\pm when $t \ll 1$, respectively, the following expansions in regions III^\pm .

Region III^+ : $t = O(1)^+$ and $u = u^+ + o(1)$ as $x \rightarrow \infty$

In this region, there are three distinct cases, depending upon α . We must first write,

$$u(x, t) = u^+ - (u^+ - u^-) \exp(-\chi(x, t)). \quad (18)$$

Then, for $\alpha \in (\frac{1}{2}, \infty)$, we have,

$$\chi(x, t) = \frac{x^2}{4t} + \log x + \frac{1}{2}(\log \pi - \log t - u^+ c_{1\alpha}) + o(1) \text{ as } x \rightarrow \infty, \quad (19)$$

with $t = O(1)^+$, while for $\alpha \in (0, \frac{1}{2})$, we have,

$$\chi(x, t) = \frac{x^2}{4t} - \frac{u^+}{2(1-2\alpha)} x^{1-2\alpha} + \log x + \frac{1}{2}(\log \pi - \log t - u^+ c_{3\alpha}) + o(1) \text{ as } x \rightarrow \infty, \quad (20)$$

with $t = O(1)^+$. In the marginal case $\alpha = \frac{1}{2}$, we obtain,

$$\chi(x, t) = \frac{x^2}{4t} + \left(1 - \frac{1}{2}u^+\right) \log x + \frac{1}{2}(\log \pi - \log t - u^+ c_{2\alpha}) + o(1) \text{ as } x \rightarrow \infty, \quad (21)$$

with $t = O(1)^+$. Here,

$$c_{1\alpha} = \int_0^\infty (1+s^2)^{-\alpha} ds, \quad (22)$$

$$c_{2\alpha} = \int_0^1 (1+s^2)^{-\frac{1}{2}} ds + \int_1^\infty \left\{ (1+s^2)^{-\frac{1}{2}} - s^{-1} \right\} ds, \quad (23)$$

$$c_{3\alpha} = \int_0^\infty \left\{ (1 + s^2)^{-\alpha} - s^{-2\alpha} \right\} ds. \tag{24}$$

Region III⁻: $t = O(1)^+$ and $u = u^- + o(1)$ as $x \rightarrow -\infty$

In this region, there are again three distinct cases. To begin with, we must write,

$$u(x, t) = u^- + (u^+ - u^-) \exp(-\bar{\chi}(x, t)), \tag{25}$$

with now, for $\alpha \in (\frac{1}{2}, \infty)$, we have,

$$\bar{\chi}(x, t) = \frac{x^2}{4t} + \log(-x) + \frac{1}{2}(\log \pi - \log t - u^- d_{1\alpha}) + o(1) \text{ as } x \rightarrow -\infty \tag{26}$$

with $t = O(1)^+$, while for $\alpha \in (0, \frac{1}{2})$,

$$\bar{\chi}(x, t) = \frac{x^2}{4t} + \frac{u^-}{2(1-2\alpha)}(-x)^{1-2\alpha} + \log(-x) + \frac{1}{2}(\log \pi - \log t - \frac{1}{2}u^- d_{3\alpha}) + o(1) \text{ as } x \rightarrow -\infty \tag{27}$$

with $t = O(1)^+$. Finally, in the marginal case $\alpha = \frac{1}{2}$, the expansion becomes,

$$\bar{\chi}(x, t) = \frac{x^2}{4t} + \left(1 + \frac{1}{2}u^-\right) \log(-x) + \frac{1}{2}(\log \pi - \log t - u^- d_{2\alpha}) + o(1) \text{ as } t \rightarrow -\infty \tag{28}$$

with $t = O(1)^+$. Here, $d_{i\alpha} = -c_{i\alpha}$ for $i = 1, 2, 3$.

We are now in a position to use the asymptotic forms derived above, as $x \rightarrow \pm\infty$, to provide the starting point from which we are able to construct the detailed asymptotic structure of the solution to (BIVP) as $t \rightarrow \infty$.

4 | ASYMPTOTIC SOLUTION AS $t \rightarrow \infty$ WITH $\alpha \in (0, \frac{1}{2})$

This section concentrates on constructing the detailed large- t structure of the solution to (BIVP) when $\alpha \in (0, \frac{1}{2})$. We begin in $x > 0$. An examination of expansion (20) with (18) shows that when $t \gg 1$ this expansion remains uniform for $x \gg t$, but fails when $x = O(t)^+$. Thus, to continue the asymptotic structure, we introduce region IV⁺, in which $x = O(t)^+$ as $t \rightarrow \infty$. It should be noted here that the form of the expansions in each spatial region which is introduced when t is large is determined by examining the form of the expansion in the neighboring region, when written in the current regions scaled coordinates.

Region IV⁺: $x = O(t)^+$ and $u = u^+ + o(1)$ as $t \rightarrow \infty$

We first introduce the scaled coordinate $y = x/t = O(1)^+$ as $t \rightarrow \infty$ in this region. It then follows from the expansion in region III⁺, when $x = O(t)^+$, that we must write:

$$u(y, t) = u^+ - (u^+ - u^-) \exp(-t\gamma_+(y, t)), \tag{29}$$

after which, on writing (3) in terms of y and t , expanding $\gamma_+(y, t)$ appropriately, and matching with the corresponding expansion in region III^+ as $y \rightarrow \infty$, we obtain (omitting details for brevity),

$$\gamma_+(y, t) = \frac{1}{4}y^2 - \frac{u^+}{2(1-2\alpha)}y^{1-2\alpha}t^{-2\alpha} + \frac{1}{2}t^{-1} \log t + H_{4+}(y)t^{-1} + o(t^{-1}) \text{ as } t \rightarrow \infty \quad (30)$$

with $y = O(1)^+$. Here, $H_{4+}(y)$ is a globally determined smooth function, which must satisfy

$$H_{4+}(y) \sim \log y + \frac{1}{2} \log \pi - \frac{1}{2}u^+c_{3\alpha} \text{ as } y \rightarrow \infty. \quad (31)$$

Correspondingly, we next introduce region IV^- , when $y = O(1)^-$ as $t \rightarrow \infty$.

Region IV^- : $x = O(t)^-$ and $u = u^- + o(1)$ as $t \rightarrow \infty$

An examination of the expansion in region III^- when, $x = O(t)^-$, determines that we must write,

$$u(y, t) = u^- + (u^+ - u^-) \exp(-t\gamma_-(y, t)) \quad (32)$$

after which we obtain, following matching with region III^- as $y \rightarrow -\infty$,

$$\gamma_-(y, t) = \frac{1}{4}y^2 + \frac{u^-}{2(1-2\alpha)}(-y)^{1-2\alpha}t^{-2\alpha} + \frac{1}{2}t^{-1} \log t + H_{4-}(y)t^{-1} + o(t^{-1}) \text{ as } t \rightarrow \infty \quad (33)$$

with $y = O(1)^-$. Again, $H_{4-}(y)$ is a globally determined smooth function, which satisfies,

$$H_{4-}(y) \sim \log(-y) + \frac{1}{2} \log \pi - \frac{1}{2}u^-d_{3\alpha} \text{ as } y \rightarrow -\infty. \quad (34)$$

An examination of expansions (30) and (33) demonstrates that they become nonuniform when $y = O(t^{-\frac{2\alpha}{1+2\alpha}})^{\pm}$ (which corresponds to $x = O(t^{\frac{1}{1+2\alpha}})^{\pm}$), respectively. Thus, to continue the asymptotic structure, we must introduce two further regions. We begin in region V^+ .

Region V^+ : $x = O(t^{\frac{1}{1+2\alpha}})^+$ and $u = u^+ + o(1)$ as $t \rightarrow \infty$

We first introduce the scaled coordinate $w = xt^{-\frac{1}{1+2\alpha}} = O(1)^+$ as $t \rightarrow \infty$ in this region. An examination of the expansion in region IV^+ then requires us to write,

$$u(w, t) = u^+ - (u^+ - u^-) \exp\left(-t^{\frac{(1-2\alpha)}{(1+2\alpha)}} \Psi^+(w, t)\right), \quad (35)$$

after which we expand in the form,

$$\Psi^+(w, t) = \Psi_0^+(w) + o(1) \text{ as } t \rightarrow \infty, \quad (36)$$

with $w = O(1)$. On substituting from (35) and (36) into Equation (3) and expanding, we obtain at leading order the equation,

$$\mathcal{N}[\Psi_0^+, w, u^+] \equiv (\Psi_0^+)'^2 + \left(\frac{u^+}{|w|^{2\alpha}} - \frac{w}{(1+2\alpha)}\right) \Psi_0^+ + \frac{(1-2\alpha)}{(1+2\alpha)} \Psi_0^+ = 0, \text{ with } w = O(1), \quad (37)$$

and

$$\Psi_0^+(w) > 0, \quad (38)$$

while matching to region IV^+ requires,

$$\Psi_0^+(w) \sim \frac{1}{4}w^2 \text{ as } w \rightarrow \infty. \quad (39)$$

The problem for $\Psi_0^+(w)$ will be completed, interactively, at a later stage in this section. However, with this in mind, we make some fundamental observations regarding Equation (37) with (38) and (39). The following result is readily established.

(R^+)

Each of the following statements hold for Equation (37)

(i) $u^+ \geq 0$: For each $w_0 > ((1 + 2\alpha)u^+)^{\frac{1}{(1+2\alpha)}}$, there exists a unique solution on $[w_0, \infty)$ which has

$$\Psi_0^+(w), \Psi_0^{+'}(w) > 0 \quad \forall w > w_0 \quad (40)$$

with

$$\Psi_0^+(w_0) = 0, \quad \Psi_0^{+'}(w_0) = \frac{w_0}{(1 + 2\alpha)} - \frac{u^+}{w_0^{2\alpha}} > 0 \quad (41)$$

and

$$\Psi_0^+(w) \sim \frac{1}{4}w^2 \text{ as } w \rightarrow \infty. \quad (42)$$

For $w_0 = ((1 + 2\alpha)u^+)^{\frac{1}{(1+2\alpha)}}$, the conditions (40) continue to hold for $w > w_0$, with now,

$$\Psi_0^+(w) = O((w - w_0)^2) \text{ as } w \rightarrow w_0^+, \quad (43)$$

while condition (42) continues to hold. Also, when $u^+ = 0$ and $w_0 = 0$, we have, exactly,

$$\Psi_0^+(w) = \frac{1}{4}w^2 \quad \forall w \geq 0. \quad (44)$$

(ii) $u^+ < 0$: For each $w_0 > -((1 + 2\alpha)(-u^+))^{\frac{1}{(1+2\alpha)}}$, there exists a unique solution on $[w_0, \infty)$ which again satisfies conditions (40) and (42), with, for $w_0 \neq 0$,

$$\Psi_0^+(w_0) = 0, \quad \Psi_0^{+'}(w_0) = \frac{w_0}{(1 + 2\alpha)} - \frac{u^+}{|w_0|^{2\alpha}} > 0, \quad (45)$$

while, for $w_0 = 0$,

$$\Psi_0^+(w) \sim -\frac{u^+}{(1 + 2\alpha)}w^{(1-2\alpha)} \text{ as } w \rightarrow 0^+. \quad (46)$$

For $w_0 = -((1 + 2\alpha)(-u^+))^{\frac{1}{(1+2\alpha)}}$, we again have (43).

The above statements in (R^+) are established by identifying the local existence and uniqueness of a solution for each initial value problem, which follows standard ODE theory, then establishing monotonicity of solutions to the initial value problem, and then using this to establish a priori bounds for the initial value problem, which allows us to infer global existence and uniqueness for the initial value problem. The far field asymptotic forms are derived directly from the ODE, making use of monotonicity. At this stage, we must leave region V^+ , and return for its completion, interactively, at a later stage. For the present, we move on to introduce region V^- .

Region V^- : $x = O(t^{\frac{1}{(1+2\alpha)^-}})$ and $u = u^- + o(1)$ as $t \rightarrow \infty$

In this region, $w = O(1)^-$ as $t \rightarrow \infty$, and it follows from the form of the expansion in region IV^- that we must write,

$$u(w, t) = u^- + (u^+ - u^-) \exp(-t^{\frac{(1-2\alpha)}{(1+2\alpha)}} \Psi^-(w, t)) \quad (47)$$

and expand as,

$$\Psi^-(w, t) = \Psi_0^-(w) + o(1) \text{ as } t \rightarrow \infty, \quad (48)$$

with $w = O(1)$. After substituting into Equation (3), when written in terms of w and t , and expanding, we obtain at leading order,

$$\mathcal{N}[\Psi_0^-, w, u^-] = 0, \text{ with } w = O(1), \quad (49)$$

and the requirement,

$$\Psi_0^-(w) > 0, \quad (50)$$

while matching to region IV^- demands that,

$$\Psi_0^-(w) \sim \frac{1}{4} w^2 \text{ as } w \rightarrow -\infty. \quad (51)$$

Again, the leading order problem must be completed, interactively, at a later stage. For the present, we may readily establish the following useful properties of Equation (49) with (50) and (51).

(R^-)

Each of the following statements holds for Equation (49)

(i) $u^- \leq 0$: For each $w_0 < -((1 + 2\alpha)(-u^-))^{\frac{1}{(1+2\alpha)}}$, there exists a unique solution on $(-\infty, w_0]$ which has

$$\Psi_0^-(w) > 0, \Psi_0^{-\prime}(w) < 0 \quad \forall w < w_0, \quad (52)$$

with

$$\Psi_0^-(w_0) = 0, \Psi_0^{-\prime}(w_0) = \frac{w_0}{(1 + 2\alpha)} - \frac{u^-}{|w_0|^{2\alpha}} < 0 \quad (53)$$

and

$$\Psi_0^-(w) \sim \frac{1}{4}w^2 \text{ as } w \rightarrow -\infty. \quad (54)$$

For $w_0 = -((1 + 2\alpha)(-u^-)^{\frac{1}{1+2\alpha}})$, the conditions (53) continue to hold for $w < w_0$, with now,

$$\Psi_0^-(w) = O((w - w_0)^2) \text{ as } w \rightarrow w_0^-, \quad (55)$$

while condition (54) continues to hold. Again, when $u^- = 0$ and $w_0 = 0$, we have, exactly,

$$\Psi_0^-(w) = \frac{1}{4}w^2 \quad \forall w \leq 0. \quad (56)$$

(ii) $u^- > 0$: For each $w_0 < ((1 + 2\alpha)u^-)^{\frac{1}{1+2\alpha}}$, there exists a unique solution on $(-\infty, w_0]$ which again satisfies conditions (52) and (54), with, for $w_0 \neq 0$,

$$\Psi_0^-(w_0) = 0, \quad \Psi_0^{-\prime}(w_0) = \frac{w_0}{(1 + 2\alpha)} - \frac{u^-}{|w_0|^{2\alpha}} < 0, \quad (57)$$

while, for $w_0 = 0$,

$$\Psi_0^-(w) \sim \frac{u^-}{(1 - 2\alpha)}(-w)^{1-2\alpha} \text{ as } w \rightarrow 0^-. \quad (58)$$

The above results in (R^-) are obtained in much the same way as described for the earlier corresponding initial value problems in (R^+) . The next, and key, region determines the selection of w_0 for regions V^\pm above, and acts as a “wavefront” region, effecting the transition from the $-$ regions to the $+$ regions. We first deal with the case when $u^+ < u^-$. In this case, as a consequence of the expansions in regions V^\pm , the transition is expected to take place locally, and we must now introduce region SW as follows.

Region $SW(u^+ < u^-)$: $w = w_0 + o(1)$ and $u = O(1)$ as $t \rightarrow \infty$

It is in this region that w_0 will be determined. We first write:

$$w = w_0 + t^{-\delta}\xi, \quad (59)$$

with $\xi = O(1)$ as $t \rightarrow \infty$ and $\delta > 0$ to be determined. On expanding,

$$u(\xi, t) = u_s(\xi) + o(1) \text{ as } t \rightarrow \infty \quad (60)$$

with $\xi = O(1)$, and substituting into (3), we find that a nontrivial leading order balance (recalling $0 < \alpha < \frac{1}{2}$) requires that,

$$\delta = \frac{1 - 2\alpha}{1 + 2\alpha}. \quad (61)$$

We note that, in terms of the original spatial coordinate x , we now have,

$$x = w_0 t^{\frac{1}{1+2\alpha}} + t^{\frac{2\alpha}{1+2\alpha}} \xi. \quad (62)$$

After substitution from (60) and (62) into (3), we obtain, at leading order, the following balances:
 (i) $u^+ + u^- > 0$

$$u'_s = \frac{1}{2w_0^{2\alpha}}(u_s - u^+)(u_s - u^-), \quad \xi \in \mathbb{R}, \quad (63)$$

where, in obtaining the factorization on the right-hand side above, we must choose,

$$w_0 = w_0^s \equiv \left(\frac{1}{2}(1 + 2\alpha)(u^+ + u^-) \right)^{\frac{1}{1+2\alpha}} > 0. \quad (64)$$

(ii) $u^+ + u^- = 0$

In this exceptional case, $w_0 = 0$ in (59), and the leading order balance changes, now requiring a rescaling, with the choice

$$\delta = \frac{1}{1 + 2\alpha}, \quad (65)$$

which dictates, in fact, that $x = O(1)$ as $t \rightarrow \infty$ in this region, in this case, with the leading order balance now giving

$$u''_s - \frac{u_s}{(1 + x^2)^\alpha} u'_s = 0, \quad x \in \mathbb{R}. \quad (66)$$

In both of the above two cases, matching with regions V^\pm , respectively, leads to the boundary conditions,

$$u_s(\xi) \rightarrow u^+ \quad \text{as } \xi \rightarrow \infty, \quad (67)$$

$$u_s(\xi) \rightarrow u^- \quad \text{as } \xi \rightarrow -\infty, \quad (68)$$

noting that x replaces ξ as the independent variable with $u^- = -u^+$ (and $u^+ < 0$) in the above conditions, when dealing with case (ii).

We begin with case (i). It is readily established (recalling that here $u^+ < u^-$) that the boundary value problem (63) with conditions (67) and (68) has a unique (up to translations in ξ) solution. In fact, this can be readily obtained, by quadrature, as,

$$u_s(\xi) = \frac{1}{2}(u^- + u^+) - \frac{1}{2}(u^- - u^+) \tanh \left(\frac{(u^- - u^+)}{4w_0^{s2\alpha}} \xi \right), \quad \xi \in \mathbb{R}. \quad (69)$$

This completes the large- t structure in this case, with the determination of w_0 in (64) allowing for the interactive completion of the structure in regions V^\pm . The principal feature is a thickening and decelerating smooth shock wave, in region SW. In terms of the original spatial variable x , the location of the shock wave is,

$$x = s(t) \sim w_0^s t^{\frac{1}{1+2\alpha}}, \quad (70)$$

with thickness,

$$\Delta_s(t) = O \left(t^{\frac{2\alpha}{1+2\alpha}} \right), \quad (71)$$

as $t \rightarrow \infty$.

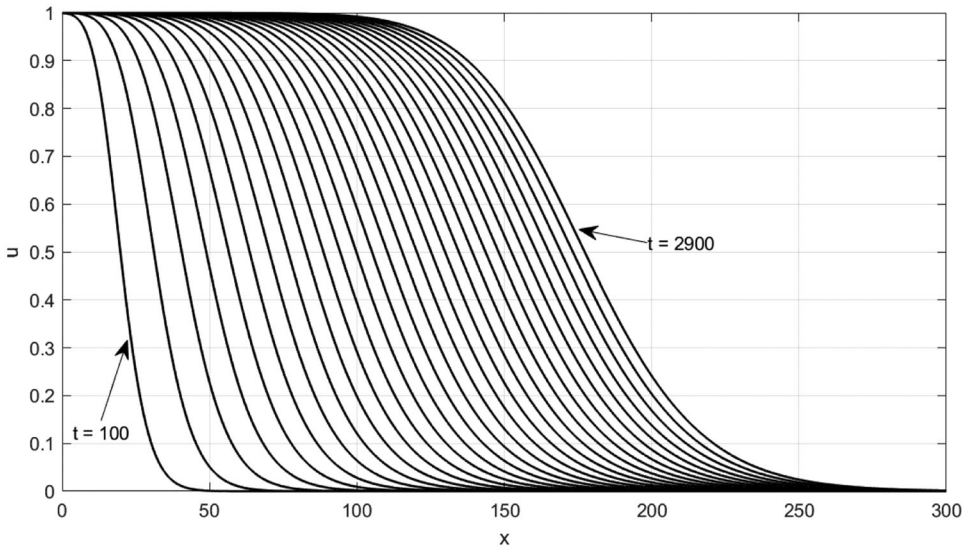


FIGURE 1 Profiles of $u(x, t)$ against x from the numerical solution of (BIVP) with $\alpha = 0.25$ and $(u^+, u^-) = (0, 1)$, at times $t = 100 - 2900$, at intervals of 100

It is instructive here to use a simple central finite difference method, which leads to second-order accuracy in space, to generate numerical solutions of (BIVP) for comparison with this asymptotic structure as $t \rightarrow \infty$. We truncate the domain of solution to $-L \leq x \leq L$ and $0 \leq t \leq T$, with $L > 0$ sufficiently large that the choice of L has no effect on the solution when $t = T$ within a chosen accuracy. We discretize the spatial domain at the N equally spaced points $x_i \equiv -L + (i - 1)\Delta x$, with $\Delta x = 2L/(N - 1)$ and $i = 1, 2, \dots, N$. At these points, (3) becomes

$$\frac{du_i}{dt} = \frac{u_{i+1} - 2u_i + u_{i-1}}{\Delta x^2} - h_\alpha(x_i) \frac{\frac{1}{2}u_{i+1}^2 - \frac{1}{2}u_{i-1}^2}{2\Delta x}, \tag{72}$$

where $u_i(t) \equiv u(x_i, t)$. We assume that $u_1(t) = u_1(0) = u^-$ and $u_N(t) = u_N(0) = u^+$. We solve this set of evolution equations using the explicit midpoint method to ensure second-order accuracy in space. We choose a timestep smaller than $\frac{1}{2}\Delta x^2$, which ensures that the method is numerically stable. In all the calculations presented in this paper, we used $\Delta x = 0.05$ and a timestep equal to $\frac{1}{4}\Delta x^2$.

Throughout the paper, we run all numerical solutions up to times when the large- t structure has evidently emerged. In Figure 1, we graph the numerical solution to (BIVP) on the (x, u) plane, when $\alpha = 0.25$ with $(u^+, u^-) = (0, 1)$, at times $t = 100 - 2900$ in increments of 100. We can readily discern the emerging, thickening, and decelerating smooth shock wave, which, at the final time is seen to be approaching the ‘‘tanh’’ profile predicted above.

In the first window of Figure 2, we consider the x -location of the point $x = x_{\frac{1}{2}}(t)$, where $u = \frac{1}{2}(u^+ + u^-) = \frac{1}{2}$, as calculated from the numerical solution, and compare this with the asymptotic location given in (70), noting that in this case, $w_0^s \approx 0.82548$. Although the numerically calculated value appears not to be in good agreement with the asymptotic behavior given by the broken line, this is deceptive because the rate of convergence is slow, of $O(t^{-\frac{1}{3}})$ as $t \rightarrow \infty$. When we fit the

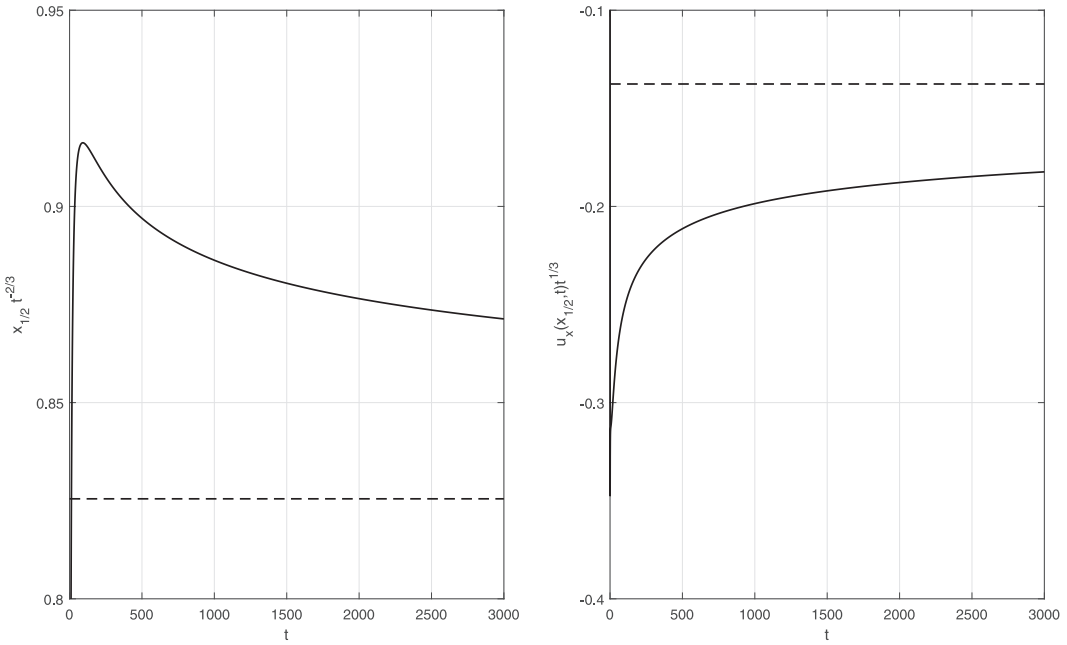


FIGURE 2 The numerically calculated position of the wavefront (left panel) and slope at the wavefront (right panel) scaled to be of $O(1)$ as $t \rightarrow \infty$

expected leading order asymptotic behavior $x_{\frac{1}{2}}(t) = w_0 t^{\frac{2}{3}} + w_1 t^{\frac{1}{3}} + w_2$ to the numerical solution for $1500 < t < 3000$, we obtain $w_0 \approx 0.8284$, in excellent agreement with w_0^S .

In the second window of Figure 2, we graph $u_x(x_{\frac{1}{2}}(t), t)^{\frac{1}{3}}$ as calculated from the numerical solution, which is a measure of the scaled front thickness. Similar remarks regarding the slow approach to the asymptotic value (shown with a broken line) apply to this quantity, as well as quantities that we plot in later graphs. The value of the limit predicted by the asymptotic theory is $t^{\frac{1}{3}} u_x(x_{\frac{1}{2}}(t), t) \rightarrow -0.1376$ as $t \rightarrow \infty$, while the fitted value is -0.1400 , again in excellent agreement.

We now move on to consider case (ii). On recasting (66) as an equivalent integral equation, it is straightforward to establish that the boundary value problem (66) with (67) and (68) has a unique solution, and this has properties,

$$u_s(0) = 0, \quad u_s(-x) = -u_s(x), \quad u'_s(x) < 0 \quad \forall x \in \mathbb{R}. \tag{73}$$

In addition,

$$u_s(x) \sim u^+ + \frac{A_\infty}{x^{2\alpha}} \exp \left\{ - \left(\frac{|u^+|}{(1 + 2\alpha)} x^{1-2\alpha} \right) \right\} \quad \text{as } x \rightarrow \infty, \tag{74}$$

with $A_\infty > 0$ being a globally determined constant, dependent on $u^+ (< 0)$ and α . This completes the large- t structure in case (ii), with the determination of $w_0 = 0$ completing interactively the structure in regions V^\pm . Again, the principal structure is a smooth shock wave, in region SW. However, in this case, the shock wave is stationary, at location $x = s(t) = 0$, and has constant

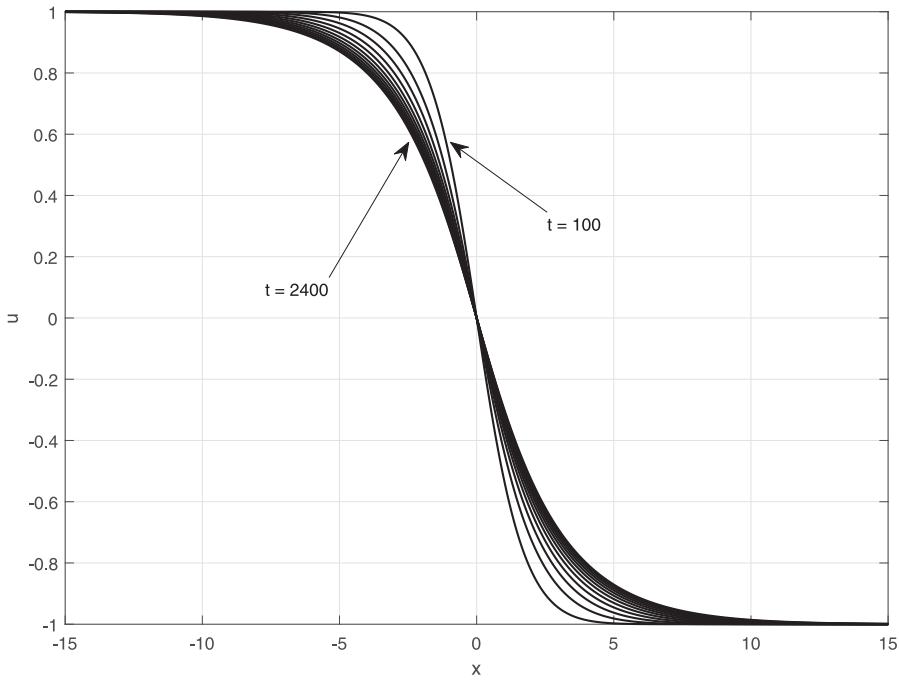


FIGURE 3 Profiles of $u(x, t)$ against x from the numerical solution of (BIVP) with $\alpha = 0.25$ and $(u^+, u^-) = (-1, 1)$, at times $t = 100 - 2400$, at intervals of 100

thickness $\Delta_s(t) = O(1)$ as $t \rightarrow \infty$. It is again instructive to make comparison with the numerical solution to (BIVP). We again take $\alpha = 0.25$, with now $(u^+, u^-) = (-1, 1)$. The numerical solution is graphed on the (x, u) plane in Figure 3 at times $t = 100 - 2400$, at intervals of 100. Convergence to a stationary, antisymmetric monotone smooth shock wave, with thickness of $O(1)$, is clearly evident.

Each case when $u^+ < u^-$ is now complete, and we move on to consider the complimentary cases, when $u^+ > u^-$. In replacement of region SW, we have the following:

Region $EW(u^+ > u^-)$: $w_0^-(u^-) + o(1) < w < w_0^+(u^+) - o(1)$ and $u = O(1)$ as $t \rightarrow \infty$

This structure follows examination of regions V^\pm , with

$$w_0^\pm(u^\pm) = \text{sgn}(u^\pm)((1 + 2\alpha)|u^\pm|)^{\frac{1}{1+2\alpha}}, \tag{75}$$

and noting that, in this case,

$$w_0^-(u^-) < w_0^+(u^+), \tag{76}$$

with the leading order boundary value problems in regions V^\pm now completed interactively by taking $w_0 = w_0^\pm(u^\pm)$, respectively. The structure in regions V^\pm requires us to expand in this region as,

$$u(w, t) = u_e(w, t) + o(u_e(w, t)) \text{ as } t \rightarrow \infty, \tag{77}$$

with $w_0^-(u^-) + o(1) < w < w_0^+(u^+) - o(1)$. After substituting from (77) into (3), expanding, and solving at leading order, together with matching to regions V^\pm , we obtain,

$$u_e(w, t) = \begin{cases} \frac{1}{(1+2\alpha)} w |w|^{2\alpha}, & |w| \geq O(1), \\ \text{sgn}(\eta) F(|\eta|) t^{-\frac{1}{2}(1-2\alpha)}, & |\eta| = O(1), \\ u_0(x) t^{-(1-\alpha)} + u_1(x) t^{-2(1-\alpha)}, & |x| = O(1). \end{cases} \quad (78)$$

Here, $\eta = w t^{\frac{1-2\alpha}{2(1+2\alpha)}}$ (which gives, in terms of the original spatial coordinate, $\eta = x t^{-\frac{1}{2}}$). The function $F : [0, \infty) \rightarrow \mathbb{R}$ is the solution to the boundary value problem,

$$F'' + \left(\frac{1}{2} \eta - \eta^{-2\alpha} F \right) F' + \frac{1}{2} (1 - 2\alpha) F = 0, \quad \eta > 0, \quad (79)$$

$$F(\eta) \rightarrow 0 \text{ as } \eta \rightarrow 0^+, \quad (80)$$

$$F(\eta) \sim \frac{1}{(1+2\alpha)} \eta^{1+2\alpha} \text{ as } \eta \rightarrow \infty. \quad (81)$$

This has a unique solution, which has a weakly singular behavior as $\eta \rightarrow 0^+$, namely,

$$F(\eta) = c\eta + \frac{c^2}{2(3-2\alpha)(1-\alpha)} \eta^{3-2\alpha} + o(\eta^{3-2\alpha}) \text{ as } \eta \rightarrow 0^+ \quad (82)$$

with $c > 0$ being a globally determined constant. In addition,

$$u_0(x) = cx \text{ and } u_1(x) = \frac{c^2}{2(1-\alpha)} \left(\int_0^x (1+\lambda^2)^{1-\alpha} d\lambda - x \right), \quad (83)$$

for $x \in \mathbb{R}$. These conclusions are established via a shooting argument from $\eta = 0$, after obtaining a straightforward monotonicity result. The local asymptotic structures are readily obtained directly from the ODE, via suitable term balancing.

The large- t structure is now complete for the cases $u^+ > u^-$, and the principal feature is a propagating expansion wave in region EW. The expansion wave is decelerating, and expanding, between the locations $x = s^\pm(t)$, where

$$s^-(t) \sim w_0^-(u^-) t^{\frac{1}{1+2\alpha}} \quad (84)$$

and

$$s^+(t) \sim w_0^+(u^+) t^{\frac{1}{1+2\alpha}} \quad (85)$$

with the expanding width being,

$$\Delta_e(t) \sim (w_0^+(u^+) - w_0^-(u^-)) t^{\frac{1}{1+2\alpha}} \quad (86)$$

as $t \rightarrow \infty$. To complete this case, we compare with numerical solutions to (BIVP). To begin, we consider the case $\alpha = 0.25$, with $(u^+, u^-) = (1, -\frac{2}{3})$. In Figure 4,

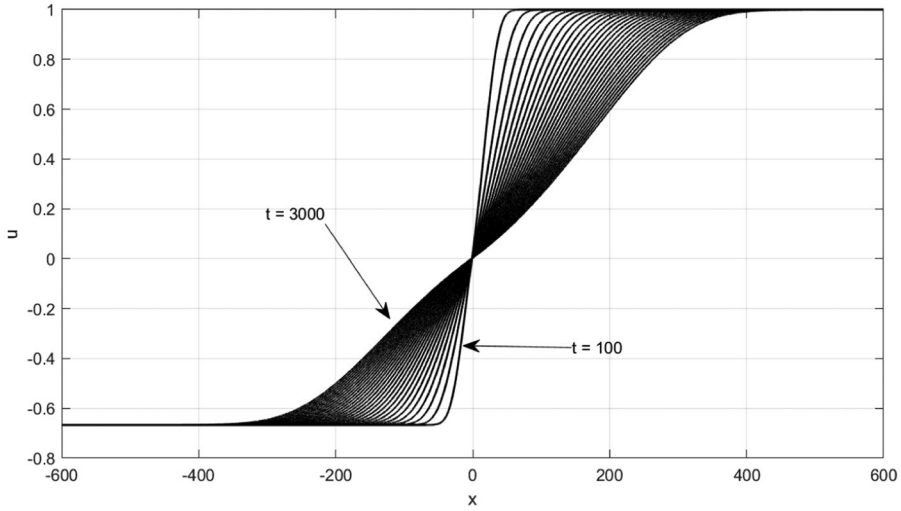


FIGURE 4 Profiles of $u(x, t)$ against x from the numerical solution of (BIVP) with $\alpha = 0.25$ and $(u^+, u^-) = (1, -\frac{2}{3})$, at times $t = 100 - 3000$, at intervals of 100

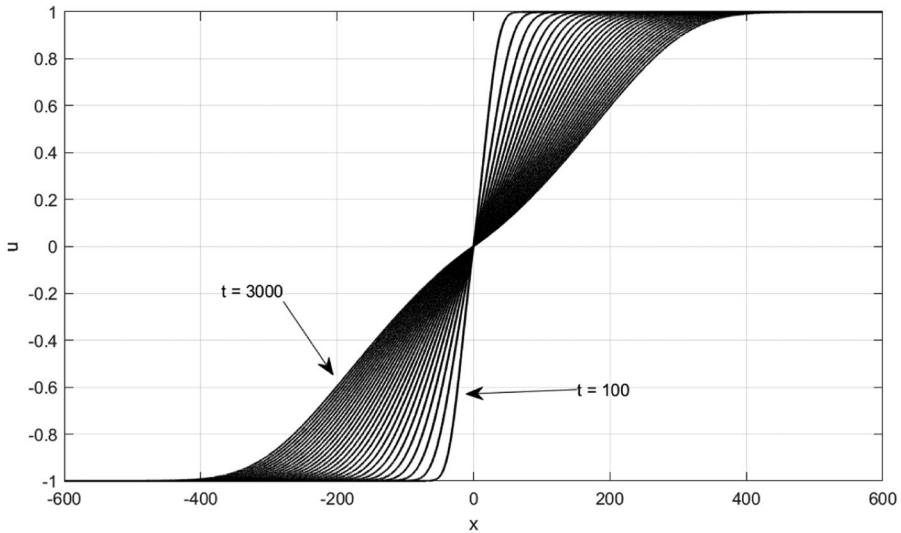


FIGURE 5 Profiles of $u(x, t)$ against x from the numerical solution of (BIVP) with $\alpha = 0.25$ and $(u^+, u^-) = (1, -1)$, at times $t = 100 - 3000$, at intervals of 100

we graph the numerical solution on the (x, u) plane at times $t = 100 - 3000$ in intervals of 100, and we see good agreement with the theory when t is large, for which, in this case, $w_0^-(-\frac{2}{3}) = -1$ and $w_0^+(1) \approx 1.31037$. Estimates calculated from the numerical solution give $w_0^-(-\frac{2}{3}) \approx -1.058$ and $w_0^+(1) \approx 1.369$. We also display an antisymmetric case in Figure 5, with again $\alpha = 0.25$, and now $(u^+, u^-) = (1, -1)$. In this case, $w_0^+(1) = -w_0^-(-1) \approx 1.31037$ and the numerical solution gives the estimate as 1.369. Agreement with the above theory, when t is large, is again good.

All cases with $(u^+, u^-) \in \mathcal{H}$ when $\alpha \in (0, \frac{1}{2})$ have now been completed, and we move on to consider the cases when $\alpha \in (\frac{1}{2}, \infty)$.

5 | ASYMPTOTIC SOLUTION AS $t \rightarrow \infty$ WITH $\alpha \in (\frac{1}{2}, \infty)$

In this section, we construct the detailed large- t structure of the solution to (BIVP) when $\alpha \in (\frac{1}{2}, \infty)$. We again begin in $x > 0$. An examination of expansion (19) establishes that, when $t \gg 1$, this expansion remains uniform for $x \gg t$ but fails when $x = O(t)^+$. Thus, to continue the asymptotic structure, we again introduce region IV^+ , which has exactly the same details as that in Section 4, except that here, expansion (30) is now replaced by,

$$\gamma_+(y, t) = \frac{1}{4}y^2 + \frac{1}{2}t^{-1} \log t + H^+(y)t^{-1} + o(t^{-1}) \text{ as } t \rightarrow \infty \quad (87)$$

with $y = O(1)^+$. Here, $H^+(y)$ is an indeterminate function in the large- t structure, being globally related, but matching to region III^+ requires,

$$H^+(y) \sim \log y - \frac{1}{2}u^+c_{1\alpha} + \frac{1}{2} \log \pi \text{ as } y \rightarrow \infty. \quad (88)$$

Similarly, we next introduce region IV^- , when $x = O(t)^-$ as $t \rightarrow \infty$, which again has exactly the same details as in Section 4, but now with expansion (33) replaced by,

$$\gamma_-(y, t) = \frac{1}{4}y^2 + \frac{1}{2}t^{-1} \log t + H^-(y)t^{-1} + o(t^{-1}) \text{ as } t \rightarrow \infty, \quad (89)$$

with, again, $H^-(y)$ indeterminate, while matching to region III^- requiring,

$$H^-(y) \sim \log(-y) - \frac{1}{2}u^-d_{1\alpha} + \frac{1}{2} \log \pi \text{ as } y \rightarrow -\infty. \quad (90)$$

An examination of expansions (87) and (89) reveals that these expansions become nonuniform, in this case, when $y = O(t^{-\frac{1}{2}})^\pm$ (which corresponds to $x = O(t^{\frac{1}{2}})^\pm$), respectively. Therefore, to complete the asymptotic structure, we must next introduce two further asymptotic regions. We begin in region V^+ .

Region V^+ : $y = O(t^{-\frac{1}{2}})^+$ and $u = O(1)$ as $t \rightarrow \infty$

In this region, we expand in the form,

$$u(w, t) = u_0^+(w) + o(1) \text{ as } t \rightarrow \infty \quad (91)$$

with now $w = xt^{-\frac{1}{2}} = O(1)^+$. After substitution into Equation (3) and expanding, we obtain at leading order,

$$u_0^{+''} + \frac{1}{2}wu_0^{+'} = 0, \quad w > 0, \quad (92)$$

with matching to region IV^+ requiring,

$$u_0^+(w) \rightarrow u^+ \text{ as } w \rightarrow \infty. \tag{93}$$

The solution to (92) with (93) is readily obtained as,

$$u_0^+(w) = u^+ + \frac{1}{2}A^+(u^+ - u^-)\operatorname{erfc}\left(\frac{1}{2}w\right), \quad w > 0, \tag{94}$$

with the free constant A_+ to be determined. We note for future reference that,

$$u_0^+(0) = u^+ - \frac{1}{2}A^+(u^+ - u^-), \quad u_0^{+'}(0) = \frac{1}{2\pi^{\frac{1}{2}}}A^+(u^+ - u^-), \tag{95}$$

while matching to region IV^+ requires,

$$H^+(y) \sim \log y + \log(\sqrt{\pi}A^+) \text{ as } y \rightarrow 0^+. \tag{96}$$

We now move on to the corresponding region in $x < 0$.

Region V^- : $y = O(t^{-\frac{1}{2}})^-$ and $u = O(1)$ as $t \rightarrow \infty$

Here, we expand as,

$$u(w, t) = u_0^-(w) + o(1) \text{ as } t \rightarrow \infty, \tag{97}$$

with $w = xt^{-\frac{1}{2}} = O(1)^-$. The details follow very closely those in region V^+ , so we do not repeat. At leading order, we obtain,

$$u_0^-(w) = u^- + \frac{1}{2}A^-(u^+ - u^-)\operatorname{erfc}\left(-\frac{1}{2}w\right), \quad w < 0, \tag{98}$$

after matching with region IV^- . Again, A^- is a free constant to be determined. We note that,

$$u_0^-(0) = u^- + \frac{1}{2}A^-(u^+ - u^-), \quad u_0^{-'}(0) = \frac{1}{2\pi^{\frac{1}{2}}}A^-(u^+ - u^-), \tag{99}$$

while matching to region IV^- requires,

$$H^-(y) \sim \log(-y) + \log(\sqrt{\pi}A^-) \text{ as } y \rightarrow 0^-. \tag{100}$$

This completes region V^- .

We note that, via Theorem 1, we can deduce that both of the constants A^+ and A^- must be strictly positive. We now require a localized region to connect region V^- to region V^+ across $x = 0$. A balancing of terms in Equation (3), and noting that this localized transition region, centered at $x = 0$, should retain the full inhomogeneous factor, together with examination of the expansions in regions V^\pm , dictates that $x = O(1)$ in this transition region, and

$$u_0^+(0) = u_0^-(0) \equiv u_T = \frac{1}{2}(u^+ + u^-) + \frac{1}{4}(A^- - A^+)(u^+ - u^-), \tag{101}$$

while we must have $u = u_T + O(t^{-\frac{1}{2}})$ as $t \rightarrow \infty$. The condition (101) provides the first relation between the constants A^\pm as,

$$A^+ + A^- = 2. \quad (102)$$

Thus, we introduce:

Region Tr: $x = O(1)$ and $u = u_T + O(t^{-\frac{1}{2}})$ as $t \rightarrow \infty$

In this region, we must expand in the form,

$$u(x, t) = u_T + t^{-\frac{1}{2}}\bar{u}(x) + o(t^{-\frac{1}{2}}) \text{ as } t \rightarrow \infty, \quad (103)$$

with $x = O(1)$. On substituting into Equation (3) and expanding, we obtain at leading order,

$$\bar{u}'' - \frac{u_T}{(1+x^2)^\alpha} \bar{u}' = 0, \quad x \in \mathbb{R}. \quad (104)$$

Matching to regions V^\pm then requires,

$$\bar{u}(x) \sim \frac{A^+}{2\pi^{\frac{1}{2}}}(u^+ - u^-)x \text{ as } x \rightarrow \infty, \quad (105)$$

$$\bar{u}(x) \sim \frac{A^-}{2\pi^{\frac{1}{2}}}(u^+ - u^-)x \text{ as } x \rightarrow -\infty. \quad (106)$$

A first integral of Equation (104) gives

$$\bar{u}'(x) = C \exp\left(u_T \int_0^x (1+\lambda^2)^{-\alpha} d\lambda\right) \quad \forall x \in \mathbb{R}, \quad (107)$$

with C being a free constant. An application of the conditions (105) and (106) then requires that C , A^+ , and A^- must satisfy the two equations,

$$C \exp\left(\pm u_T \int_0^\infty (1+\lambda^2)^{-\alpha} d\lambda\right) = \frac{A^\pm}{2\pi^{\frac{1}{2}}}(u^+ - u^-). \quad (108)$$

Solution of these two equations, using (102), then gives,

$$C = \frac{1}{2\pi^{\frac{1}{2}}}(u^+ - u^-) \operatorname{sech}\left(\frac{1}{2}u_T \int_{-\infty}^\infty (1+\lambda^2)^{-\alpha} d\lambda\right), \quad (109)$$

and

$$A^+ - A^- \exp\left(u_T \int_{-\infty}^\infty (1+\lambda^2)^{-\alpha} d\lambda\right) = 0. \quad (110)$$

We now observe that u_T and both A^\pm are determined by the three simultaneous, nonlinear, algebraic equations given in (101), (102), and (110), in terms of the given parameters u^\pm and α . To examine these equations, it is convenient to introduce the new constants,

$$\Sigma = A^+ + A^-, \quad (111)$$

$$\Delta = A^+ - A^-. \quad (112)$$

We then have immediately, from (102), that

$$\Sigma = 2, \quad (113)$$

after which Equations (101) and (110) become,

$$(2 + \Delta) \exp(-u_T I) - (2 - \Delta) = 0, \quad (114)$$

$$u_T = \frac{1}{2}(u^+ + u^-) - \frac{1}{4}\Delta(u^+ - u^-), \quad (115)$$

with

$$I = \int_{-\infty}^{\infty} (1 + \lambda^2)^{-\alpha} d\lambda > 0. \quad (116)$$

After substituting from (115) for u_T into (114), we obtain a scalar equation for Δ , namely,

$$\exp\left(\frac{1}{2}(u^+ + u^-)I\right)(2 - \Delta)(2 + \Delta)^{-1} = \exp\left(\frac{1}{4}(u^+ - u^-)I\Delta\right). \quad (117)$$

It is straightforward to establish that Equation (117) has a unique solution, say $\Delta = \Delta^*$, which depends on each of u^\pm and α . In particular,

$$\Delta^* \in \begin{cases} (0, 2) & \text{for } u^+ > -u^-, \\ (-2, 0) & \text{for } u^+ < -u^-, \\ 0 & \text{for } u^+ = -u^-. \end{cases} \quad (118)$$

In terms of Δ^* , we now have, via (109), (111), and (112),

$$A^+ = \frac{1}{2}(2 + \Delta^*), \quad (119)$$

$$A^- = \frac{1}{2}(2 - \Delta^*), \quad (120)$$

with

$$C = \frac{1}{2\pi^{\frac{1}{2}}}(u^+ - u^-)\operatorname{sech}\left(\frac{1}{2}u_T(u^+ - u^-)I\right), \quad (121)$$

while u_T is given by (115) with $\Delta = \Delta^*$. An integration of (107) finally gives,

$$\bar{u}(x) = \bar{u}(0) + C(u^+, u^-, \alpha) \int_0^x \exp\left(u_T(u^+, u^-, \alpha) \int_0^s (1 + \lambda^2)^{-\alpha} d\lambda\right) ds \quad \forall x \in \mathbb{R}, \quad (122)$$

with $C(u^+, u^-, \alpha)$ and $u_T(u^+, u^-, \alpha)$ as given in (121) and (115), respectively, with the value of $\bar{u}(0)$ requiring the determination of, and matching to, terms of $O(t^{-\frac{1}{2}})$ in regions V^\pm , which we do not

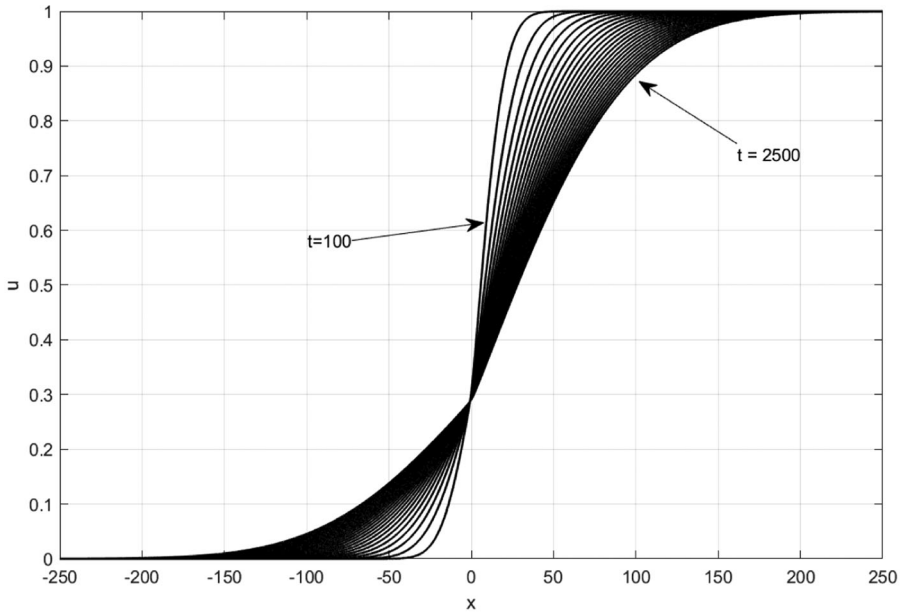


FIGURE 6 Profiles of $u(x, t)$ against x from the numerical solution of (BIVP) with $\alpha = 1$ and $(u^+, u^-) = (1, 0)$, at times $t = 100 - 2500$, at intervals of 100

pursue here. It is of interest to note the special case when $u^+ = -u^-$. Simple calculations from above then give, explicitly, $\Delta^* = 0$, and thus $u_T = 0$, while $A^+ = A^- = 1$ and $C = u^+ / \sqrt{\pi}$, with,

$$\bar{u}(x) = \bar{u}(0) + \frac{u^+}{\sqrt{\pi}}x \quad \forall x \in \mathbb{R}. \tag{123}$$

We observe that in this special case, we can also infer from Corollary 1 that $u(x, t)$ is an odd function of $x \in \mathbb{R}$, and thus we may conclude that $\bar{u}(0) = 0$ in (123).

The asymptotic structure of the solution to (BIVP) as $t \rightarrow \infty$ is now complete for all cases with $(u^+, u^-) \in \mathcal{H}$ when $\alpha > \frac{1}{2}$. The principal feature is the diffusion scale front regions V^\pm , when $x = O(t^{\frac{1}{2}})$, connected by the localized steady region, when $x = O(1)$. To conclude this case, we compare the large- t structure developed above with illustrative numerical solutions of (BIVP). For the numerical solution of (BIVP), we set $\alpha = 1$. First, we consider $(u^+, u^-) = (1, 0)$, and the numerical solution is illustrated on the (x, u) plane in Figure 6, where regions V^\pm , which have thickness $O(t^{\frac{1}{2}})$, and Tr , which has $O(1)$ thickness, are readily seen emerging for t large. As a check on numerical accuracy, we have from the asymptotic solution that $u(0, t) = u_T + O(t^{-\frac{1}{2}})$, with $u_T \approx 0.288$, while the numerical solution gives $u_T \approx 0.2852$. In Figure 7, we graph $u(0, t)$ against t as calculated from the numerical solution, which shows good agreement with the $O(t^{-\frac{1}{2}})$ decay to u_T as $t \rightarrow \infty$, in accord with the asymptotic theory.

We next consider the case $(u^+, u^-) = (0, 1)$, with the numerical solution illustrated in Figure 8.

In this case, the region Tr is more pronounced, with more asymmetry between regions V^\pm , and from the asymptotic solution, we again have $u(0, t) = u_T + O(t^{-\frac{1}{2}})$, with now $u_T \approx 0.952$, while the numerical solution gives $u_T \approx 0.9402$. In Figure 9, we graph $u(0, t)$ against t as obtained

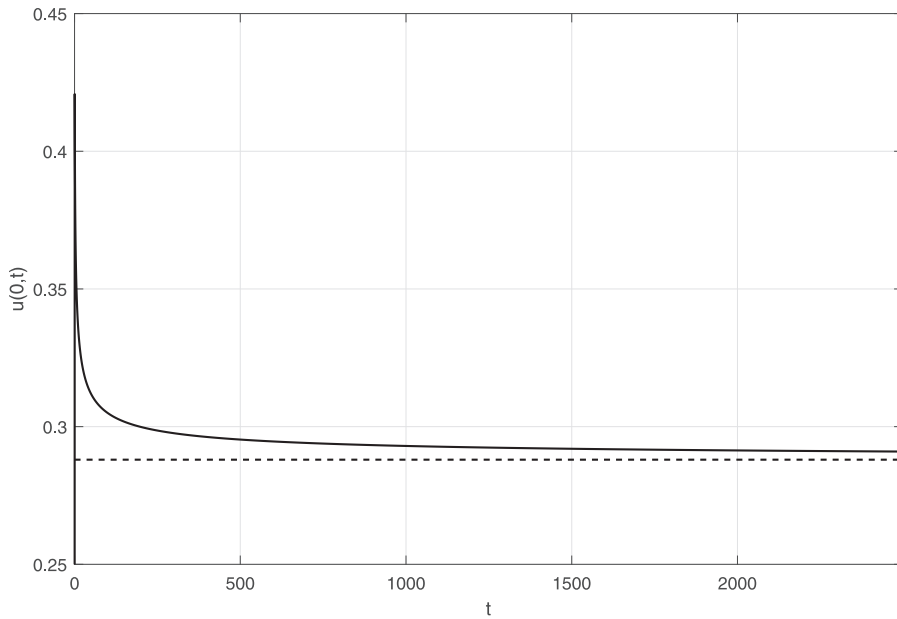


FIGURE 7 $u(0, t)$ against t as calculated from the numerical solution to (BIVP) with $\alpha = 1$ and $(u^+, u^-) = (1, 0)$. The dashed line is at the limiting value given by the asymptotic theory

from the numerical solution to (BIVP), which illustrates the $O(t^{-\frac{1}{2}})$ approach to the limit u_T as predicted by the asymptotic theory.

Finally, in Figures 10 and 11, we illustrate the numerical solution for the cases $(u^+, u^-) = (1, -1)$ and $(u^+, u^-) = (-1, 1)$, respectively. In each case, the antisymmetry of the profiles about the u -axis is evident. It should also be noted that the two cases are close, but not exactly, antisymmetric images of each other. This is in line with the asymptotic theory.

We now move on to consider the final, marginal, case when $\alpha = \frac{1}{2}$. In particular, it is of principal interest to determine whether this marginal case follows the shock/expansion wave structures seen when $0 < \alpha < \frac{1}{2}$ or the diffusion dominated structures seen when $\alpha > \frac{1}{2}$.

6 | ASYMPTOTIC SOLUTION AS $t \rightarrow \infty$ WITH $\alpha = \frac{1}{2}$

This section develops the asymptotic solution to (BIVP) as $t \rightarrow \infty$, in the marginal case when $\alpha = \frac{1}{2}$. We again begin in $x > 0$, with an examination of expansion (21) determining that, when $t \gg 1$, this expansion remains uniform for $x \gg t$, but fails when $x = O(t)^+$. Therefore, to continue the asymptotic structure, we again introduce region IV^+ , which has the same details as in Section 4, except that now expansion (30) is here replaced by,

$$\gamma_+(y, t) = \frac{1}{4}y^2 + \frac{1}{2}(1 - u^+)t^{-1} \log t + G^+(y)t^{-1} + o(t^{-1}) \text{ as } t \rightarrow \infty \quad (124)$$

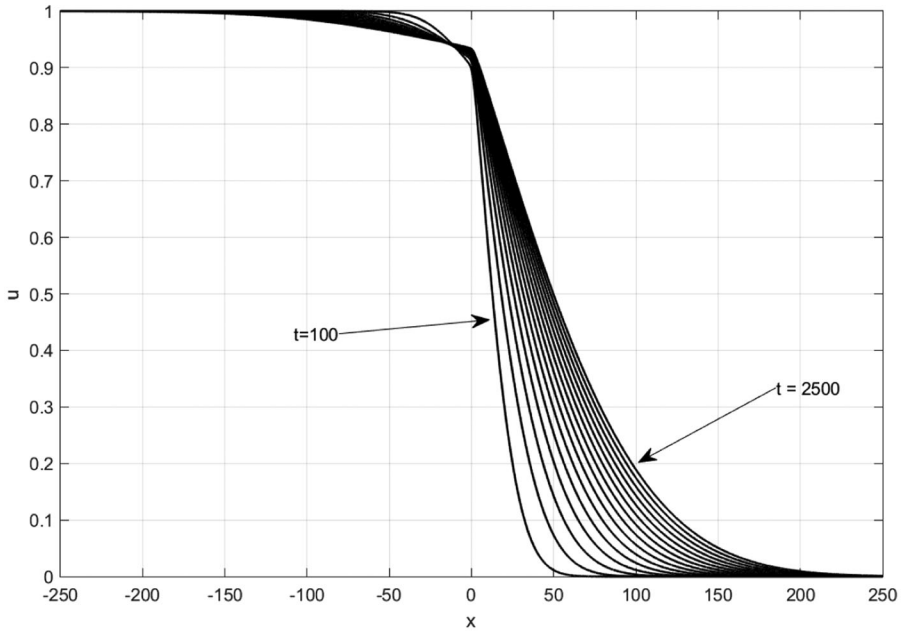


FIGURE 8 Profiles of $u(x, t)$ against x from the numerical solution of (BIVP) with $\alpha = 1$ and $(u^+, u^-) = (0, 1)$ for $t = 100 - 2500$ at intervals of 100

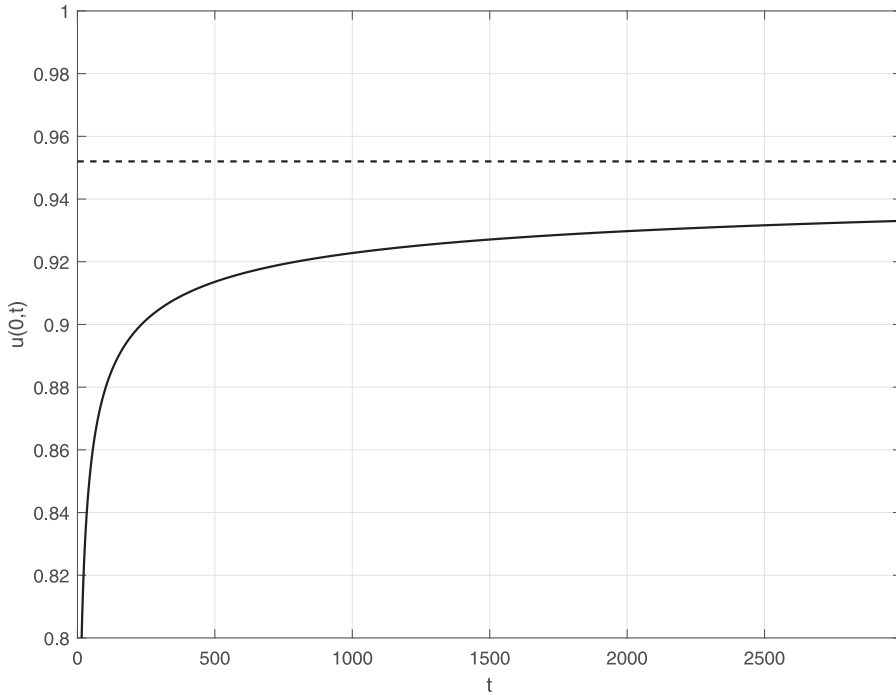


FIGURE 9 $u(0, t)$ against t from the numerical solution of (BIVP) with $\alpha = 1$ and $(u^+, u^-) = (0, 1)$. The dashed line represents the value u_T as given by the asymptotic theory

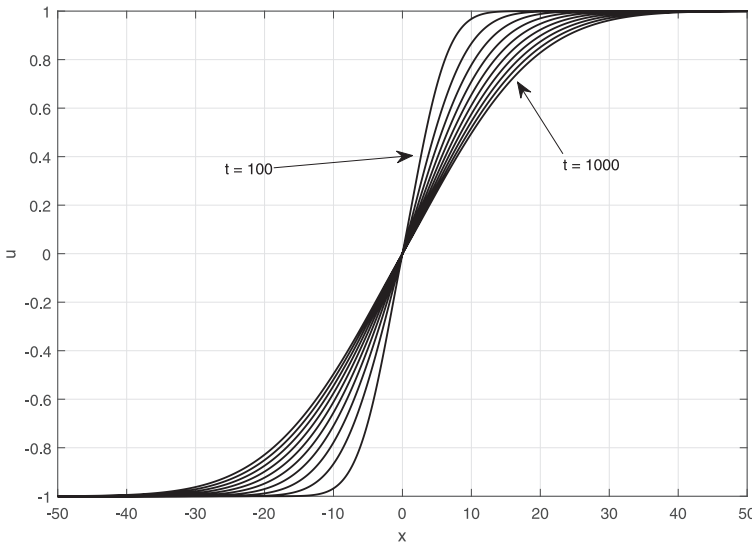


FIGURE 10 Profiles of $u(x, t)$ against x from the numerical solution of (BIVP) with $\alpha = 1$ and $(u^+, u^-) = (1, -1)$ for $t = 100 - 1000$ at intervals of 100

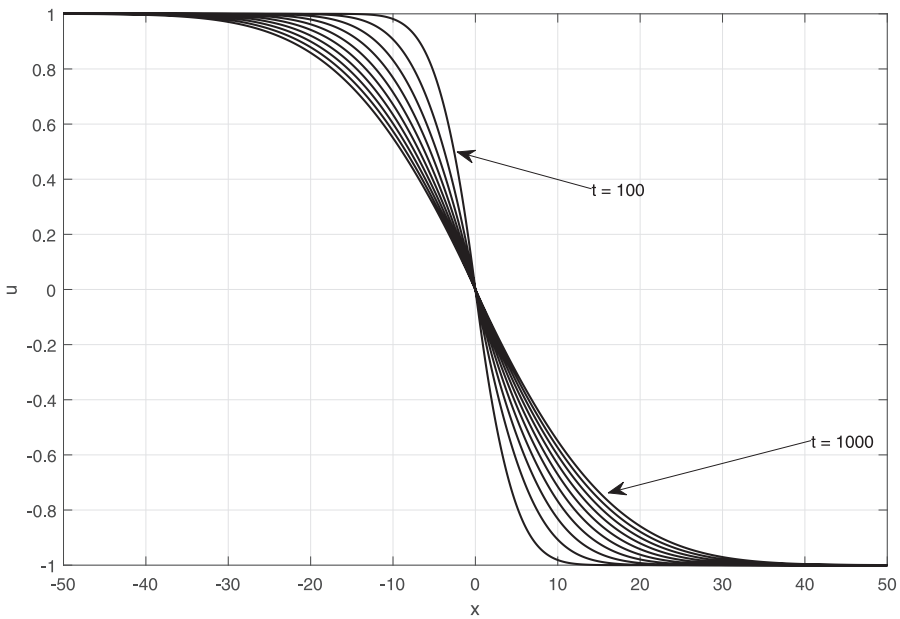


FIGURE 11 Profiles of $u(x, t)$ against x from the numerical solution of (BIVP) with $\alpha = 1$ and $(u^+, u^-) = (-1, 1)$ for $t = 100 - 1000$ at intervals of 100

with $y = O(1)^+$. Here, $G^+(y)$ is an indeterminate function in the large- t structure, but matching with region III^+ requires,

$$G^+(y) \sim \left(1 - \frac{1}{2}u^+\right) \log y - \frac{1}{2}(u^+c_{2\alpha} - \log \pi) \text{ as } y \rightarrow \infty. \tag{125}$$

Similarly, we next introduce region IV^- , when $x = O(t)^-$ as $t \rightarrow \infty$, which has exactly the same details as in Section 4, but now expansion (33) is replaced by,

$$\gamma_-(y, t) = \frac{1}{4}y^2 + \frac{1}{2}(1 + u^-)t^{-1} \log t + G^-(y)t^{-1} + o(t^{-1}) \text{ as } t \rightarrow \infty, \quad (126)$$

with, again, $G^-(y)$ indeterminate, whilst matching to region III^- requires,

$$G^-(y) \sim (1 + \frac{1}{2}u^-) \log(-y) - \frac{1}{2}(u^- d_{2\alpha} - \log \pi) \text{ as } y \rightarrow -\infty. \quad (127)$$

Expansions (124) and (126) become nonuniform when $y = O(t^{-\frac{1}{2}})^\pm$, respectively. Thus, we must introduce a transition region, when, as in Section 5, $w = xt^{-\frac{1}{2}} = O(1)^\pm$ as $t \rightarrow \infty$. We label this as region Tr . There are a number of subregions to consider. We begin first in regions Tr^\pm . For brevity, we give essential details only. At leading order, we have simply,

$$u(w, t) = u^\pm + O(t^{-\Gamma}) \text{ as } t \rightarrow \infty \quad (128)$$

with $w = O(1)^\pm$, respectively, and $\Gamma > 0$ to be determined. There are now two cases to consider. First, we address the expansive case, when $u^+ > u^-$.

$u^+ > u^-$: In this case, expansions (128) become nonuniform when $w = w^\pm \pm o(1)$ ($w^+ > w^-$), respectively, where two passive corner regions are required to locally connect with the main expansive region, in which $w \in (w^- + o(1), w^+ - o(1))$ and $u = O(1)$ as $t \rightarrow \infty$. Here, w^\pm both depend upon u^\pm and are determined interactively. As the corner regions are passive, we omit their details (and record that the corner regions will fix Γ in (128)) and proceed directly into the main expansive region, which we label as region EW . In region EW , we have,

$$u(w, t) = u_e(w) + O(t^{-\frac{1}{2}}) \text{ as } t \rightarrow \infty, \quad (129)$$

for $w \in (w^- + o(1)^+, w^+ - o(1)^+)$ with $u_e : \mathbb{R} \rightarrow \mathbb{R}$ satisfying,

$$u_e(w) = -u_e(-w) \quad \forall w \in \mathbb{R}. \quad (130)$$

Here, u_e is the solution of the boundary value problem (EVP), namely,

$$u_e'' + (\frac{1}{2}w - w^{-1}u_e)u_e' = 0, \quad w > 0, \quad (131)$$

$$u_e(0) = 0, \quad (132)$$

$$u_e(w) \rightarrow \infty \text{ as } w \rightarrow \infty. \quad (133)$$

It is straightforward to establish (via a shooting and monotonicity argument) that (EVP) has a solution, which is unique. Moreover, it is readily shown that the solution has the following properties,

$$u_e'(w) > 0 \quad \forall w \geq 0, \quad (134)$$

$$u_e(w) = \frac{1}{2}w^2 + 1 + O(e^{-w}) \text{ as } w \rightarrow \infty. \quad (135)$$

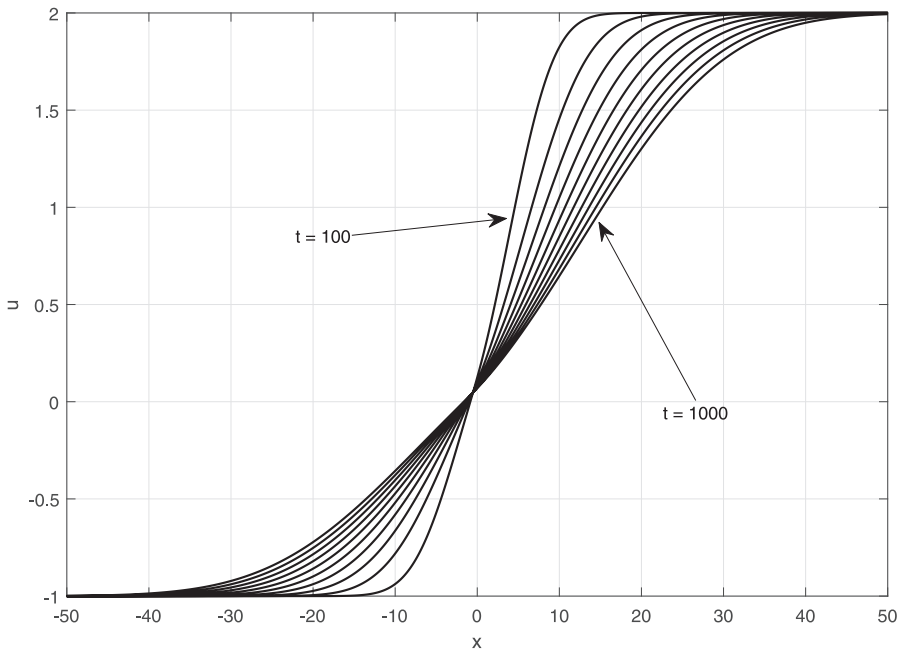


FIGURE 12 Profiles of $u(x, t)$ against x from the numerical solution of (BIVP) with $\alpha = 1/2$ and $(u^+, u^-) = (2, -1)$ for $t = 100 - 1000$ at intervals of 100

We can now match expansion (129) to the respective edge regions, which requires that w^+ and w^- are the respective, unique, solutions to the two algebraic equations,

$$u_e(w^\pm) = u^\pm. \tag{136}$$

We note that in this case, $w^+ > w^-$, via (134). This completes region *EW* in the cases where $0 \notin [w^-, w^+]$. In the remaining cases, we must introduce a final localized region when $w = O(t^{-\frac{1}{2}})$ ($x = O(1)$), with $u = o(1)$, as $t \rightarrow \infty$. For convenience in what follows, we denote $u_e'(0)$ by $A_e > 0$. In this final region, which we label as region **loc**, we obtain the expansion (omitting straightforward details),

$$u(x, t) = A_e x t^{-\frac{1}{2}} + A_e^2 \left(\int_0^x (1 + s^2)^{\frac{1}{2}} ds \right) t^{-1} + O(t^{-\frac{3}{2}}) \text{ as } t \rightarrow \infty, \tag{137}$$

with $x = O(1)$. The structure is now complete in the expansive case. We have seen that the principal feature is that of a decelerating expansion wave, now between the locations $x = \Sigma_\pm(t)$, where,

$$\Sigma_\pm(t) \sim w^\pm t^{\frac{1}{2}} \text{ as } t \rightarrow \infty. \tag{138}$$

We complete this case with some numerical illustrations when $\alpha = \frac{1}{2}$. In Figure 12,

we show the numerical solution to (BIVP) in the case $(u^+, u^-) = (2, -1)$, while the antisymmetric case $(u^+, u^-) = (1, -1)$ is illustrated in Figure 13. In each case, excellent agreement is shown

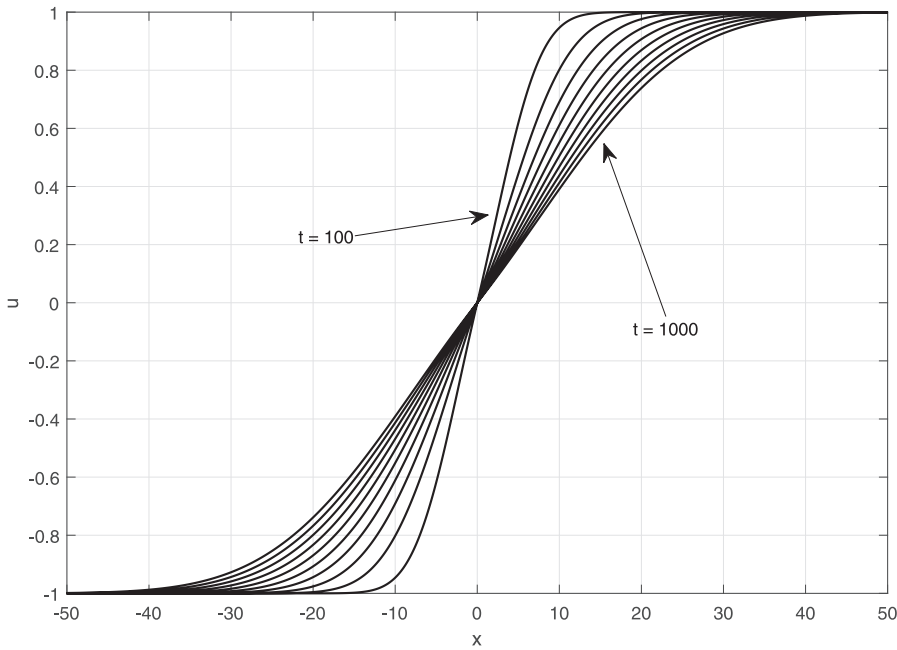


FIGURE 13 Profiles of $u(x, t)$ against x from the numerical solution of (BIVP) with $\alpha = 1/2$ and $(u^+, u^-) = (1, -1)$ for $t = 100 - 1000$ at intervals of 100

with the above asymptotic structure, with the principle feature in each case being an expansion wave on an $O(t^{\frac{1}{2}})$ length scale.

$u^+ < u^-$: In this compressive case, for brevity, we restrict attention to the situation when $u^- = -u^+ \equiv u_\infty > 0$, with the remaining cases commented on at the end of the subsection. In this case, it follows from Theorem 1 and Corollary 1, that the solution to (BIVP) is an odd, monotone decreasing, function of $x \in \mathbb{R}$ at each $t > 0$, and thus we need only construct the structure in $w > 0$. We find that there are two subcases to consider.

The first is for $u_\infty > 1$. We recall from (128) that in region Tr^+ , when $w = O(1)^+$, we have the expansion,

$$u(w, t) = -u_\infty + \bar{u}(w)t^{-\Gamma} + o(t^{-\Gamma}) \text{ as } t \rightarrow \infty, \quad (139)$$

which matches with region IV^+ , at leading order, as $w \rightarrow \infty$. At next order, we obtain the problem,

$$\bar{u}'' + \left(\frac{1}{2}w + u_\infty w^{-1}\right)\bar{u}' + \Gamma\bar{u} = 0, \quad w > 0, \quad (140)$$

with the requirements,

$$\bar{u}(w) > 0, \quad \bar{u}'(w) < 0 \quad \forall w > 0, \quad (141)$$

which follows from Theorem 1, together with matching to region IV^+ , which requires,

$$\bar{u}(w) = O(e^{-\frac{1}{4}w^2}) \text{ as } w \rightarrow \infty. \quad (142)$$

It is readily established (again via a shooting approach) that this problem has a one parameter family of solutions, parameterized by $a_0 > 0$, and which has,

$$\bar{u}(w) \sim a_0 w^{-(u_\infty-1)} \text{ as } w \rightarrow 0^+, \tag{143}$$

and,

$$\bar{u}(w) \sim a_\infty(a_0)w^{(2\Gamma-(1+u_\infty))}e^{-\frac{1}{4}w^2} \text{ as } w \rightarrow \infty, \tag{144}$$

with $a_\infty(a_0) > 0$, depending upon a_0 , and a_0 to be determined interactively. We must now move on to region *SW*, a final region containing a stationary shock wave. In this region, $x = O(1)^+$ and $u = O(1)^-$ as $t \rightarrow \infty$, and thus we expand in the form,

$$u(x, t) = u_s(x) + o(1) \text{ as } t \rightarrow \infty. \tag{145}$$

At leading order, we obtain the boundary value problem,

$$u_s'' - \frac{u_s}{(1+x^2)^{\frac{1}{2}}}u_s' = 0, \quad x > 0, \tag{146}$$

$$u_s(0) = 0, \quad u_s'(0) < 0, \tag{147}$$

$$u_s(x) \sim -u_\infty + a_0x^{-(u_\infty-1)} \text{ as } x \rightarrow \infty, \tag{148}$$

with the latter condition coming from matching to the expansion in region *Tr*⁺, which also requires,

$$\Gamma = \frac{1}{2}(u_\infty - 1) > 0. \tag{149}$$

We label this boundary value problem as (SBVP). We consider (SBVP) via a shooting method from $x = 0$. Thus, we consider the associated initial value problem consisting of the ODE (146), with initial conditions,

$$u_s(0) = 0, \quad u_s'(0) = -\delta_0, \tag{150}$$

with $\delta_0 > 0$ fixed. This initial value problem has a unique global solution, which is monotone decreasing in $x \geq 0$, and has,

$$u_s(x) \sim -c(\delta_0) + d(\delta_0)x^{-(u_\infty-1)} \text{ as } x \rightarrow \infty, \tag{151}$$

with $c, d : \mathbb{R}^+ \rightarrow \mathbb{R}$ being both continuous and positive, and c being monotone. In addition, asymptotic solutions to the initial value problem when δ_0 is small and large, establish that,

$$c(\delta_0) \rightarrow 1^+ \text{ as } \delta_0 \rightarrow 0^+, \tag{152}$$

and

$$c(\delta_0) \sim \sqrt{2}\delta_0^{\frac{1}{2}} \text{ as } \delta_0 \rightarrow \infty. \tag{153}$$

We can now return to (SBVP), for which it now follows that a unique solution exists for each $u_\infty > 0$, which corresponds to the solution of the above initial value problem with $\delta_0 = \delta^*$, where δ^* is the unique positive solution to the algebraic equation,

$$c(\delta^*) = u_\infty, \quad (154)$$

after which condition (148) determines a_0 as,

$$a_0 = d(\delta^*) > 0. \quad (155)$$

Finally, we can perform detailed matching between region Tr^+ and region IV^+ , which is achieved with the requirement that, via (144),

$$G^+(y) \sim \frac{1}{2} \log y + \log(2u_\infty/a_\infty(a_0)) \text{ as } y \rightarrow \infty. \quad (156)$$

This completes the structure when $u_\infty > 1$.

The final case has $0 < u_\infty \leq 1$. In this case, the stationary shock region is absent, and replaced by a weak and passive adjustment region when $x = O(1)$. First, in region Tr^+ , we now expand as,

$$u(w, t) = \hat{u}(w) + o(1) \text{ as } t \rightarrow \infty, \quad (157)$$

with $w = O(1)^+$. The leading order problem is then given by the boundary value problem,

$$\hat{u}'' + \left(\frac{1}{2}w + \hat{u}w^{-1}\right)\hat{u}' = 0, \quad w > 0, \quad (158)$$

$$\hat{u}(0) = 0, \quad \hat{u}'(0) < 0, \quad (159)$$

$$\hat{u}(w) = -u_\infty + O(e^{-\frac{1}{4}w^2}) \text{ as } w \rightarrow \infty. \quad (160)$$

We refer to this boundary value problem as (DBVP). It is straightforward to establish that the solution to (DBVP) is monotone decreasing in $w \geq 0$, and can be obtained by shooting from $w = 0$, with $\hat{u}'(0) < 0$ as the shooting parameter. A numerical investigation determines that for each $0 < u_\infty \leq 1$, the boundary value problem (DBVP) has a unique solution, and in particular, this solution has,

$$\hat{u}(w) = -c_*w + \frac{1}{2}c_*^2w^2 + O(w^3) \text{ as } w \rightarrow 0^+, \quad (161)$$

and,

$$\hat{u}(w) \sim -u_\infty + c_\infty w^{-(1+u_\infty)} e^{-\frac{1}{4}w^2} \text{ as } w \rightarrow \infty, \quad (162)$$

with the two positive constants c_* and c_∞ depending continuously on u_∞ , while matching to region IV^+ requires,

$$G^+(y) \sim (1 + u_\infty) \log y + \log(2u_\infty/c_\infty) \text{ as } y \rightarrow 0^+. \quad (163)$$

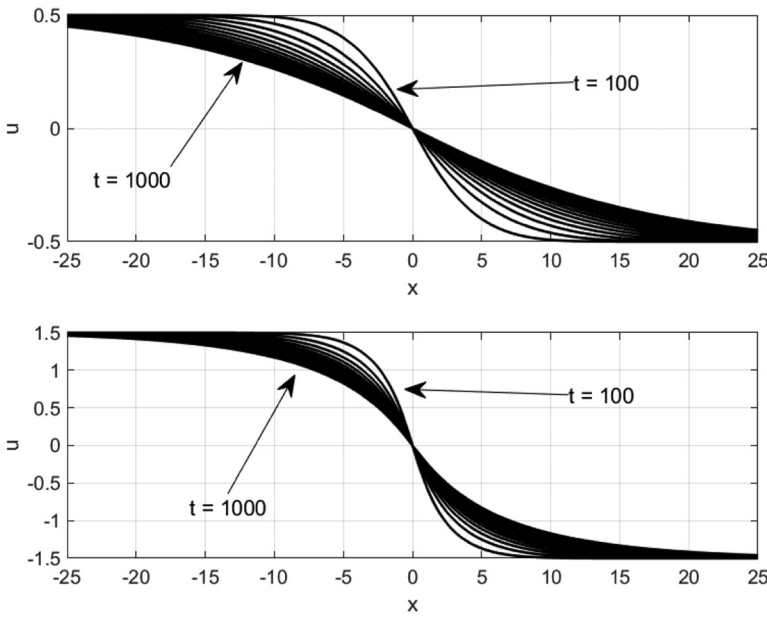


FIGURE 14 Profiles of $u(x, t)$ against x from the numerical solutions of (BIVP) with $\alpha = \frac{1}{2}$ and in the top window $u_\infty = \frac{1}{2}$, while in the bottom window, $u_\infty = \frac{3}{2}$, for $t = 100 - 1000$ at intervals of 100

Finally, we move into the weak, localized adjustment region A , in which $x = O(1)^+$, and we must expand in the form,

$$u(x, t) = -c_* x t^{-\frac{1}{2}} + \Phi(x) t^{-1} + o(t^{-1}) \text{ as } t \rightarrow \infty, \tag{164}$$

with $x = O(1)^+$. The leading order problem is then given by,

$$\Phi'' = c_*^2 \frac{x}{(1 + x^2)^{\frac{1}{2}}}, \quad x > 0, \tag{165}$$

$$\Phi(0) = 0, \quad \Phi(x) \sim \frac{1}{2} c_*^2 x^2 \text{ as } x \rightarrow \infty, \tag{166}$$

with the second condition coming from matching with region Tr^+ . The solution to this boundary value problem is readily obtained as,

$$\Phi(x) = Ax + c_*^2 \int_0^x (1 + s^2)^{\frac{1}{2}} ds \quad \forall x > 0, \tag{167}$$

with $A > 0$ a constant whose determination requires the construction, and matching to, higher-order terms in region Tr^+ . For brevity, we do not pursue this further. The structure is now complete in this final case. When $u_\infty > 1$, the key feature is a stationary smooth shock wave about $x = 0$, while, when $0 < u_\infty \leq 1$, this changes to a stationary diffusion scale front about $x = 0$. We comment that a combination of these two key features arises in the non-antisymmetric cases depending on the values of u^\pm in relation to the critical values ± 1 , respectively. We finish with some illustrative numerical solutions to (BIVP) in this case. In the top window of Figure 14, we present the numerical solution to (BIVP) when $u_\infty = 0.5$.

As predicted by the asymptotic theory, the large- t structure involves the formation of an anti-symmetric diffusion front, spreading on a length scale of $O(t^{\frac{1}{2}})$. Finally, in the bottom window of Figure 14, we present the numerical solution to (BIVP) when $u_\infty = \frac{3}{2}$. In this case, as again predicted by the asymptotic theory, the key large- t structure is a stationary smooth shock wave, on an $O(1)$ length scale.

All cases in the marginal situation, when $\alpha = \frac{1}{2}$, have now been dealt with. We conclude that the large- t structure depends critically on u^+ and u^- , and can involve as the key feature, either a smooth shock wave, an expansion wave, or a diffusion front.

7 | DISCUSSION

This paper has considered the Riemann problem (BIVP), for a spatially inhomogeneous generalized Burgers equation, with spatial inhomogeneity characterized by the parameter $\alpha > 0$, with the spatial rate of decay of the nonlinear sound speed being algebraic with increasing distance, and increasing with increasing α . The Riemann data parameters are (u^+, u^-) , and need only be considered with $(u^+, u^-) \in \mathcal{H}$. The principal focus has been on constructing the detailed large- t asymptotic structure of the solution to (BIVP), and thereby identifying the key attracting features in each case, as $t \rightarrow \infty$. There are three distinct cases. First, for weaker spatial decay rates, with $\alpha \in (0, \frac{1}{2})$, the principal large- t structure is an algebraically decelerating and weakly thickening, smooth shock wave when $u^+ < u^-$, and conversely, a smooth decelerating and algebraically expanding expansion wave when $u^+ > u^-$. The precise details are given in Section 4. For stronger spatial decay rates, with $\alpha \in (\frac{1}{2}, \infty)$, the principal large- t structure switches to a diffusion dominated front on the diffusion length scale of $O(t^{\frac{1}{2}})$, in all cases of the Riemann parameters. This is detailed in Section 5. Finally, the marginal case, when $\alpha = \frac{1}{2}$, has a principal large- t structure which develops overall on a length scale of $O(t^{\frac{1}{2}})$, and can be either a smooth decelerating and weakly thickening shock wave, an algebraically expanding expansion wave, or a diffusion front, depending crucially on the Riemann parameters. This case is presented in Section 6. Throughout, the asymptotic theory is supported by careful numerical solutions to (BIVP). More general qualitative theory for (BIVP) is given in the second of this pair of papers (MNII). To conclude, we observe that for modifications of (BIVP) with, specifically, more general “single hump,” continuous and piecewise smooth forms for the spatial inhomogeneity function $h_\alpha : \mathbb{R} \rightarrow [0, \infty)$, comparison with the present theory indicates that the approach developed here will again be applicable, with minor modifications. In particular, we anticipate that $h_\alpha(x) = O(|x|^{-1})$ as $|x| \rightarrow \infty$ is the critical decay rate, in the sense that faster decay rates inhibit smooth shock wave or expansion wave formation, with error function type diffusion-fronts forming when t is large, while slower decay rates lead to decelerating and thickening smooth shock waves or decelerating expansion waves forming when t is large. As determined here, the marginal case may involve any of these structures, depending on the Riemann parameters.

DATA AVAILABILITY STATEMENT

The data that support the findings of this study are openly available in Zenodo at <https://zenodo.org/record/6817204#.YsvqgHbMKUk>, reference number 10.5281/zenodo.6817204.

ORCID

John C. Meyer  <https://orcid.org/0000-0003-0708-1088>

REFERENCES

1. Leach JA, Needham DJ. Matched Asymptotic Expansions in Reaction-Diffusion Theory. London: Springer Monographs in Mathematics; 2003.
2. Crighton DG, Scott JF. Asymptotic solutions of model equations in nonlinear acoustics. *Philos Trans R Soc Lond A*. 1979;292(1389):102-133.
3. Scott JF. The long time asymptotics of the solutions to the generalized Burgers equation. *Proc R Soc Lond*. 1981;A373:443-556.
4. Nimmo JJC, Crighton DG. Geometrical and diffusive effects in nonlinear acoustic propagation over long ranges. *Philos Trans R Soc A*. 1986;320:1-35.
5. Lee-Bapty IP, Crighton DG. Nonlinear wave motion governed by the modified Burgers equation. *Philos Trans R Soc A*. 1987;323:173-209.
6. Hammerton PW, Crighton DG. Approximate solution methods for nonlinear acoustic propagation over long ranges. *Proc R Soc Lond A*. 1989;426:125-152.
7. Leach JA. The large-time solution of Burgers' equation with time dependent coefficients. I The coefficients are exponential functions. *Stud Appl Math*. 2016;136(2):163-188.
8. Suleiman FB, Leach JA, Needham DJ. The large-time solution of Burgers' equation with time dependent coefficients. II Algebraic coefficients. *Stud Appl Math*. 2016;137:273-303.
9. Le U, Pelinovsky DE, Pouillet P. Asymptotic stability of viscous shocks in the modular Burgers equation. *Nonlinear*. 2021;34:5979-6016.
10. Whitham GB. *Linear and Nonlinear Waves*. New York: Wiley; 1974.
11. Rudenko OV, Soluyan SL. *Theoretical Foundations of Nonlinear Acoustics*. New York: Plenum; 1977.
12. Rao CS, Nath S. A study of separable solutions of a generalized Burgers equation. *Stud Appl Math*. 2015;134(4):403-419.
13. Vaganan BM, Jeyalakshmi T. Generalized Burgers equations transformable to the Burgers equation. *Stud Appl Math*. 2011;127(3):2011-220.
14. Rao CS, Yadav MK. Solutions of a nonhomogeneous Burgers equation. *Stud Appl Math*. 2010;124(4):411-422.
15. Engu Satyanarayana MA, Murugan V. Large time asymptotics with error estimates to solutions of a forced Burgers equation. *Stud Appl Math*. 2016;138(2):185-204.
16. Vaganan BM. Cole-Hopf transformations for higher dimensional Burgers equations with variable coefficients. *Stud Appl Math*. 2012;129(3):300-308.
17. Naumkin PI, de J Villela-Aguilar J J. Asymptotics of solutions to periodic problem for the Korteweg-de Vries-Burgers equation. *Stud Appl Math*. 2022;149(2):523-536.
18. Meyer JC, Needham DJ. The Riemann problem for a generalised Burgers equation with spatially decaying sound speed. II General qualitative theory. Arxiv. 2022;2209.04832.

How to cite this article: Needham DJ, Meyer JC, Billingham J, Drysdale C. The Riemann problem for a generalized Burgers equation with spatially decaying sound speed. I Large-time asymptotics. *Stud Appl Math*. 2023;1-33. <https://doi.org/10.1111/sapm.12561>